地震研究所彙報
Bull. Earthq. Res. Inst.
Univ. Tokyo
Vol. 76 (2001) pp. 391-415

Electric Field Variations Related to Seismic Swarms

Yukio Fujinawa[1]*, Kozo Takahashi[2]**, Takumi Matsumoto[1], Hiroshi Iitaka[3], Takuya Doi[3], Takeshi Nakayama[4]**, Toyoaki Sawada[4] and Hideo Sakai[5]

[1] National Research Institute for Earth Science and Disaster Prevention
[2] Communications Research Laboratory
[3] National Institute of Advanced Industrial Science and Technology
[4] Disaster Prevention Research Institute, Kyoto University
[5] Toyama University
(** former affiliation)

Abstract

We have been observing subsurface electric field variations using specially designed antenna with a long casing pipe in borehole (Ultra-Long-Electrode Measurement : ULEM) at 12 sites in the central part of Japan since 1989. Analyses of electromagnetic field variation data around the times of several seismic activities, particularly during seismic swarms, indicate that the electric field anomalies correlate well with crustal activity around the site. Field changes appeared in the DC, ULF, and ELF/VLF bands ; the ELF/VLF bands did not always correlate with other bands, but were limited to the most active period. Electric signals associated with a seismic swarm are detected locally within 100 km from the network. Detectability is very heterogeneous, and selectivity of signal detection is largely attributed to the degree of hydraulic connectivity between the source generation zone and the site. The anomalies could be observed more clearly using the borehole antenna than by sensors on the ground surface, probably because of the shorter distance to the source zone, as well as the large length for the sensors to respond to field variations in the heterogeneous media. The field change anomalies may be caused by electric-kinetic effects induced by variations of the confined water circulation regime in association with earthquake occurrence. It is probable that pore water pressure changes preceding and during earthquakes can be detected by an electromagnetic field sensor embedded in the deep borehole near the path of water circulation around faults.

Key words : groundwater motion, earthquake, forecast, electric field, precursor

1. Introduction

The fluid-phase is presently of interest in an attempt to understand the complex physico-chemical process of earthquake occurrence. Fluids may play important roles in long-term structural evolution, fault creeping, and fault ruptures (e.g. Wakita *et al.*, 1987 ; Scholz, 1990 ; Hickman *et al.*, 1995). Ground water levels and chemical content have been measured in quantities that provide evidence to suggest the existence of changes in the ground water regime before earthquakes. There are numerous reports of ground water changes before earthquakes (e.g. Rikitake, 1976). In this report, we provide a different approach to this problem : through electromagnetic measurements.

Reports have been accumulating to suggest that electromagnetic field variations are induced in association with ground water movement (e.g. Ishido and Mizutani, 1981 ; Park *et al.*, 1993 ; Bernard and Le Mouel, 1996). Ground water movement was attributed to geomagnetic anomalies at the time of an extensive seismic swarm at Matsushiro in Nagano prefecture, on the basis of an electro-kinetic model (Mizutani *et al.*, 1976). The magnetic anomalies observed in association with the 1989 M_L 7.1 Lowa Prieta earthquake (Fraser-Smith *et al.*, 1990) were ex-

* e-mail : fujinawa@bosai.go.jp (3-1, Tennodai, Tsukuba, Ibaraki, 305-0006 Japan)

plained on the basis of Byerlee's fault rupture model (Byerlee, 1993). The model assumes that seals between compartments rupture, resulting in transient magnetic field variations.

However, there are no well-organized observations that confirm an intrinsic correlation between the crustal fracture process and electromagnetic field changes, and thus verify that the method works for investigations of ground water movement in the crust. The previous documentation has many shortcomings, with the result that it is impossible to evaluate whether or not the result is scientifically founded. We need a framework for this kind of investigation that would satisfy widely approved evaluation criteria such as proposed by the IASPEI subcommittee (Wyss, 1991).

Here, we present analyses of electric field observation data obtained by a very sensitive special sensor over more than ten years to demonstrate that there are electric field anomalies associated with seismic swarms. In the evaluation of correlation each item in the guidelines of the IASPEI subcommittee was considered as a working criterion. Characteristic electromagnetic field variations have been observed only in and around the geothermal zones at the time of crustal activities, leading to the inference that ground water movement related with the earthquake occurrence on the order of 10^{-3} cm/s can be efficiently detected by electromagnetic measurement.

2. Measurement Method and Observations

Electromagnetic field observation stations have been constructed in central Japan since 1988, and twelve observation sites are now in operation (Fig. 1). A borehole antenna (Fujinawa and Takahashi, 1990) is used at all sites to measure the vertical electric field by means of a casing pipe in a deep borehole, based on the original idea of Takahashi and Takahashi (1989) (Fig. 2). The steel casing pipe functions as a monopole of the antenna in conductive substance, and copper wire buried underground surrounding the casing pipe serves as the antenna reflector. An exception is the ocean bottom antenna between Ito city and Izu-Oshima measuring horizoutal component (OIO in Fig. 1).

Within the low frequency limit, the borehole can be viewed as an ultra-long electrode (ULE) immersed in the Earth. The input voltage in the detector is the weighted average of the electric potential along the casing pipe. The weighting coefficient is proportional to the inverse of the resistivity and the width of each layer. For instance, if there is an electric field change at any layer in contact with the pipe, the change can be sensed by the sensor system. A practical advantage is that this sensor can detect any electric field change at arbitrary point along the pipe. Though we cannot ascertain the layer at which the change is occurring (Honkura, 1998), the sensor can provide valuable data to indicate the approximate 2-D positions of the source. This type of measurement (Ultra Long Electrical Measurement: ULEM) has been shown to be very efficient for detecting underground anomalous signals even under conditions of high urban noise levels (Fujinawa and Takahashi, 1996).

We selected three specific frequency bands, : DC (DC to 0.7 Hz), ULF (0.01 to 0.7 Hz), and ELF/VLF (1 kHz to 9 kHz) for observations (Fujinawa and Takahashi, 1990 ; Fujinawa *et al.*, 1992). These frequency bands were selected by considering the regulations that govern radio frequencies in Japan, and the reported anomalous changes. However, it does not imply that higher frequency bands are not useful (e. g. Gokhberg *et al.*, 1987 ; Park *et al.*, 1993 ; Popov *et al.*, 1989; Parrot *et al.*, 1993; Hayakawa and Fujinawa, 1994). The average dynamic ranges for recording are, $\pm$50 mV, $\pm$5 mV, and 0-7 mV, for the DC, ULF, and ELF/VLF bands, respectively. The amplifier gain at a site was adjusted after the test observations. So the dynamic ranges are not the same at all of the sites, but the differences are not substantial. All of the whole instruments were calibrated every 1.5 months.

Raw signals have been recorded for the DC and ULF bands, and an envelope of amplitude for the ELF/VLF band due to the limited capacity of the available data transmission. Digitized data for those signals were transmitted to Tsukuba (TKB) (Fig. 1), the central station of the network, at midnight. The sampling interval of the digitized signals is about 1.5 sec, which is sufficient to reproduce electric field fluctuations in those bands.

Five sites (HAS, CKR, NAG, KOF, and SAG) in the network were additionally equipped with a waveform recording system for the pulse-like ELF/VLF band signals (VPS), with a sampling interval of 50

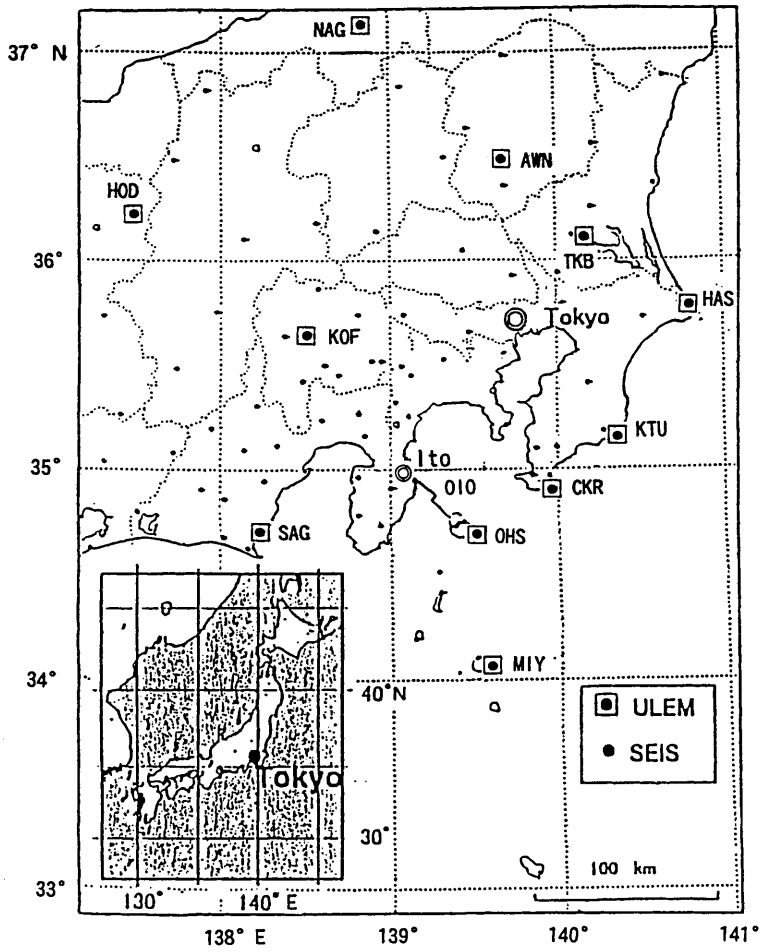

Fig. 1. Locations of electro-magnetic field observation sites in central Japan. A borehole antenna 150 to 1,200 m long was used as the principal sensor at eleven sites : Hasaki (HAS), Katsuura (KTU), Tsukuba (TKB), Chikura (CKR), Awano (AWN), Izu-Oshima (OHS), Miyakejima (MIY), Nagaoka (NGO), Koufu (KOF), Sagara (SAG), and Hodaka (HOD). Mutually perpendicular short dipoles 20 to 60 m long were used for the horizontal component of the electric field, together with three-component induction-type magnetometers for five sites (HAS, CKR, KOF, NAG, and SAG). In addition, an ocean-bottom antenna about 33 km long was constructed between Ito-City and Izu-Oshima Island (OIO). The network has been in operation since 1988, and the sites were selected on the basis of several geological conditions. Specifically, HOD, AWN, OHS, MIY, and HOD are in and around a geothermal region with active volcanoes. The small dots (SEIS) indicate the seismic observation sites of the Kanto-Tokai seismic network (Matsumura *et al.*, 1988).

kHz and a record length of 70 ms (Fujinawa *et al.*, 1997 ; Fujinawa *et al.*, 2001 a). Time synchronization at site is accomplished to the level of 1 μ sec using a GPS clock at each site. The arrival time data of VPS enable us to determine the source position of the signals. The signal location data are expected to provide clues about the generation mechanism of VPS.

The observation sites are situated at different places from the geological standpoints. Many of the sites (AWN, OSH, MYK, OIO, and HOD) are in a geothermal zone. Almost all of the wells are associated with ground water measurement (HAS, CKR, AWN), hot water pumping (OSH, HOD), or natural gas testing (NAG). The exceptions are sites TKB and SAG for strain-measurement, and MIY and KTU for ground tilt measurements. The monopoles of antenna as casing pipes or cables were not constructed for our purposes, but for their original use. Electric instruments were installed when funds were available, so the observation periods differ. The oldest site is TKB, which commenced observations in March 1989. The newest site is OIO, which began observations in October 1999.

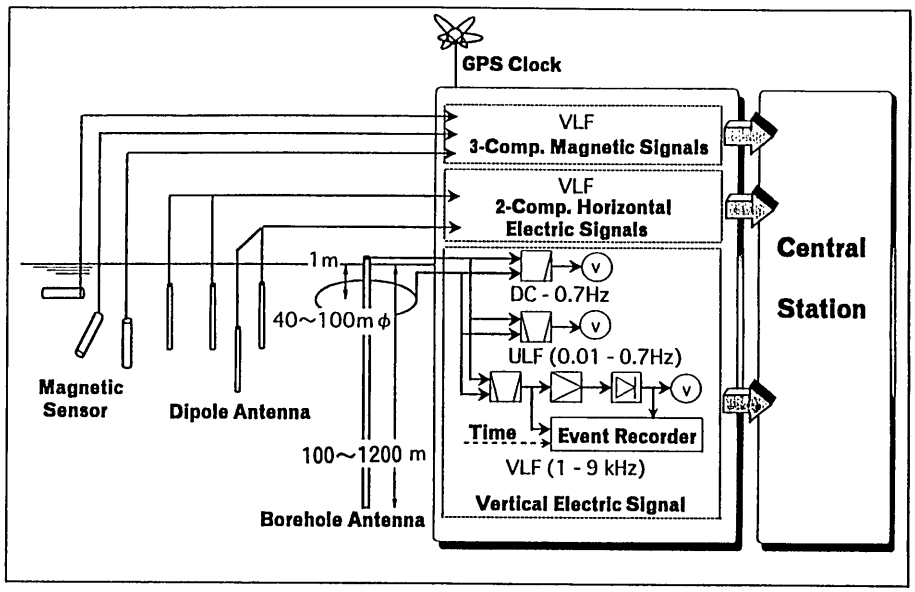

Fig. 2. Schematic diagram of multiple-component electromagnetic field observations. The electric field is measured by a pair of horizontal dipoles 8 m long with a span of 10 to 50 m, and with a vertical monopole of 100 to 1,200 m long surrounded by wire with a radius of 5 to 50 m buried at a depth of about 1 m. The magnetic field is measured by three induction-type magnetometers (BF-6, EMI) installed perpendicularly to each other. The triggered data in three electrical and magnetic field components are transmitted to a central station once a night. There are triggered recording devices for ELF/VLF band events at five sites (HAS, CKR, KOF, NAG, and SAG).

Except for occasional problems with the electrical equipment caused by severe lightning strikes, the systems have been providing high-quality data almost continuously. The circuit to protect against surging voltage has been progressively refined to reduce malfunctions due to lightning, which is almost the only cause of instrumental breakdown. The system is now satisfactorily robust for work under moderate return strokes. The lead cables have flexible steel coverings to prevent chewing by animals. Calibration includes measuring the impedance between the antenna monopole and the reflector, and measuring the amplifier gain. The impedance between the antenna monopole and reflector has been almost constant, probably because of the long time lapse after the casing pipes were installed. Strip-chart recording has been used to produce back-up data. The paper for recording the chart at the site is changed at the calibration times.

The recording parameter for the DC component was adjusted when there was signal over-scaling. A long period of observation has suggested that geophysical events only induce over-scaling in the DC band. Sufficiently long enough observation at many sites indicates that the measurements have been providing reliable data for electric field measurements to investigate crustal activities and to evaluate anomalous electric field changes as a precursor of earthquakes and volcanic eruptions.

3. Results

We have analyzed the electric field variations at times of eminent crustal activities by comparing them with records from normal stages. Here, we focus primarily on electric field anomalies at times of seismic swarms that occurred near the observation. We demonstrate that electric field anomalies in association with a seismic swarm are most probably caused by a ground water circulation change.

For any phenomenon to provide reliable information to forecast earthquakes, it is essential that that phenomenon have an intrinsic relationship with the earthquake process. Numerous scientific reports claim explicitly or implicitly that various phenomena are precursory phenomena. However, it is generally not possible to confirm these assertions because of the practical impossibility of a double-check. Moreover, the experiments were basically conducted without sufficient attention given to guideline needed for this kind of research. The most system-

atic criteria for scientific evaluations of earthquake precursors were presented by the IASPEI Sub-Commission on Earthquake Prediction (Wyss, 1991). The criteria are composed of data quality, explicit presentation of anomalies, association rule of anomalies with subsequent earthquakes, and the general properties assumed for precursor phenomena. Experiments are recommended to satisfy those criteria so that any reported anomalies will be accepted as relevant phenomena.

It is not easy to conduct experiments that strictly satisfy all of these criteria ; none were accepted out of 26 nominations (Wyss, 1991). However, it is also true that the criteria consist of items that seem reasonable enough to be used at least as working guidelines. We conducted our experiments taking those criteria into account as much as possible to investigate whether or not electric field variations are associated with earthquake occurrences. This report demonstrates that there is a significant correlation between electric field anomalies and earthquake swarms. The results also provide evidence to resolve points raised in serious debates over electromagnetic phenomena as precursors, (e.g. Lighthill, 1996 ; Geller, 1996) especially those of the Seismic Electric Signals (SES) claimed by Varotsos *et al.* (1996). The guidelines are proposed to refine several points.

3.1 Normal State

First, we describe the quality of the data, focusing on the record during a normal state without crustal activities. The largest obstacle when investigating precursors is noises from human activities and natural causes (e.g. Park *et al.*, 1993). The recording parameters were determined by trial and error after an experimental observational period of about one month ; the background noise level for the DC channel was subsequently almost a flat line, and about one-tenth of the saturation level for the ULF and the ELF/VLF bands in the monitoring record during the normal state. We tentatively assumed the normal period as one during which there are no appreciable seismic or volcanic eruption activities around the site.

An example of a record of a normal state is shown in Fig. 3 at the site HOD on 5 August 1998. The background noise levels N for the three frequency bands at this site were :

$$N_{DC} \sim 0.1\,\mathrm{mV} \quad (1\,a)$$

$$N_{ULF} \sim 0.1\,\mathrm{mV} \quad (1\,b)$$

$$N_{VLF} \sim 0.7\,\mathrm{mV} \quad (1\,c)$$

If the electric field is uniform along the casing pipe, the background noise strengths are 0.25μV/m (DC), 0.25μV/m (ULF), and 1.8μV/m (VLF). The VLF component is usually due to atmospherics, and thought to be very concentrated in the surface region, suggesting a several times larger strength near the surface compared to 1.8μV/m. The noise levels for the DC and the ULF bands have remained virtually constant since the beginning of the observations, but the level of the ELF/VLF component at HOD increased abruptly in February 1997 (Takahashi *et al.*, 2000). Before the increase, the noise level was about 0.2 mV in the ELF/VLF band. The contaminated new noise maintained a nearly constant amplitude for time period of order a day. The property enables us to discriminate this kind of noise without difficulty.

The noise levels of the ULF and DC bands at almost all sites were nearly the same as at HOD. However, larger urban noise appeared at sites in and around urban areas, such as Kofu, due to human activities. These sites have a smaller dynamic range. We distinguish such urban noise from the temporal evolution of noise levels depending on working hours and the weekly calendar.

The largest civil noises in this country are due to electric power lines, electronic facilities, and electricity-driven trains. Normal records of the vertical component show practically no discernible disturbances of a train origin at most sites for the chosen monitoring parameters, in contrast to the horizontal measurements (Fujinawa and Takahashi, 1996). This kind of noise, if present, can be easily discriminated on the ground diurnal changes and appearance at very precise times following time tables. Electric power lines are the greatest noise sources. The frequency bands were chosen to minimize this power line component by combining low-pass and high-pass filters. This selection may sacrifice the frequency window for detecting possible anomalies. However, the performance of the filters is satisfactory for our purpose and assures a sufficiently large

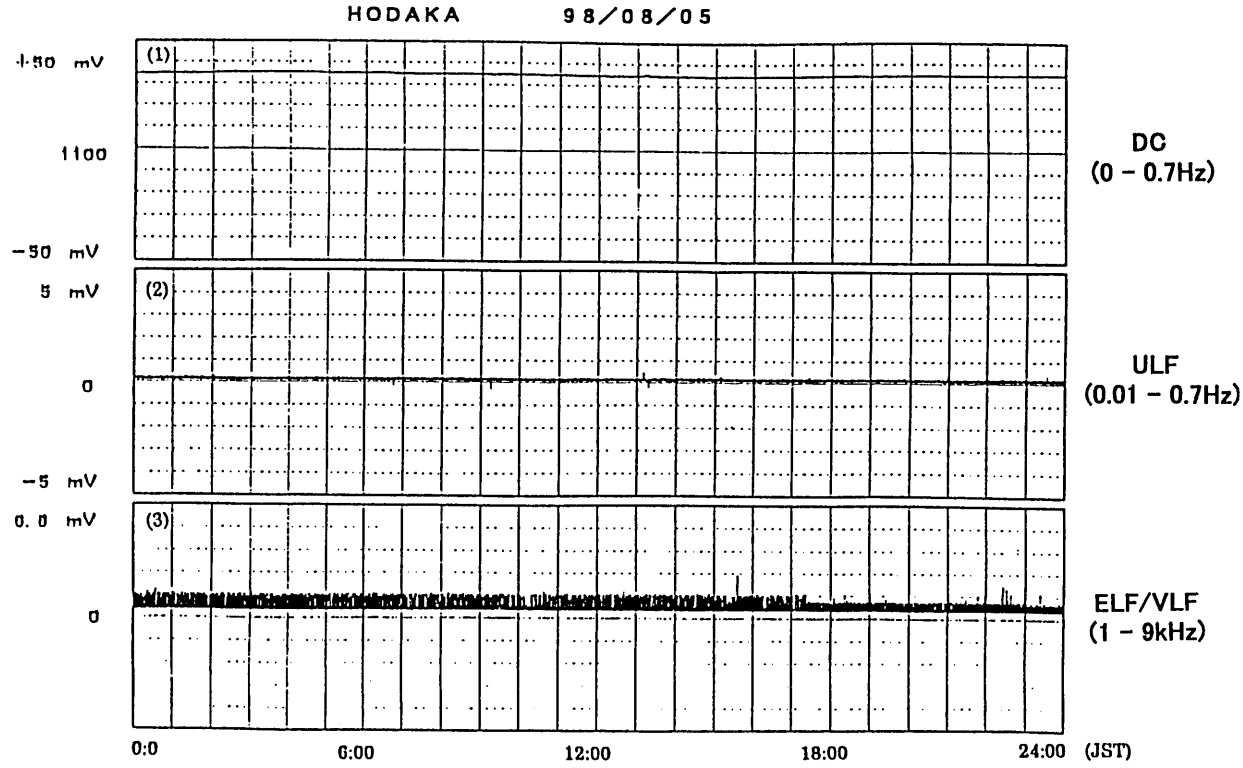

Fig. 3. An example of monitoring records in the normal state of the vertical electric field observation on 6 August 1998 at Hodaka. The DC component (0 to 0.7 Hz, upper section) has an almost flat curve for the selected recording parameters. Noise levels are less than 1/50 at full scale in the ULF band (0.01 to 0.7 Hz, middle section), and 1/20 in the ELF/VLF band (1 kHz to 9 kHz, lower section), respectively. The almost constant level signals of about 1 mV in the ELF/VLF channel (lower section) are due to urban noise at HAD starting from December 1997.

S/N for monitoring.

The choice of recording parameters for the intensity and frequency range is also based on results obtained prior to 1988 (e.g. Gokhberg *et al.*, 1987). Our long experience indicates that almost all meaningful signals are well above most of the natural and urban noise levels in our measurements. Two dominant noises except those previously described were lightning return strokes and those that occurred at the time of instrument calibrations. The return strokes that occurred near the site caused a saturation in the records for a few hours (Takahashi *et al.*, 2000). However, most extraneous surge voltages were removed by a special anti-surge circuit. The protection circuit was developed by one of the authors (Kozo Takahashi) using several zener diodes and based on numerous experiences of instrument breakdowns. Remote atmospherics never appear in the DC, or ULF bands, but they are included in the ELF/VLF band. They are generally buried in background noise in the strength record, as in Fig. 3-(3). Therefore, it is easy to discriminate the noise from nearby atmospherics based on a typical pattern of evolution with a maximum duration of a few hours. The ELF/VLF band is composed of pulse-like signals of different duration (VPS). Each VPS can also be verified as to whether or not it is of atmospherics origin based on the source location data (Fujinawa *et al.*, 1997) and the provided lightning return stroke information (Franklin Japan Inc.).

Geomagnetic disturbances are another source of large natural noises. However, they are much weaker than atmospherics. We can know whether or not the observed anomalies are of geomagnetic origin using data for the geomagnetic disturbance that is available on the website of the Communications Research Laboratory. Fig. 4 illustrates the effects of severe geomagnetic disturbances that reached 200 nT at Kakioka on 6 August 1988 (JST). The sensed strength was 0.2 mV for the ULF bands in our measurements (HOD in Fig. 4), which is about twice the original background noise level. Geomagnetic dis-

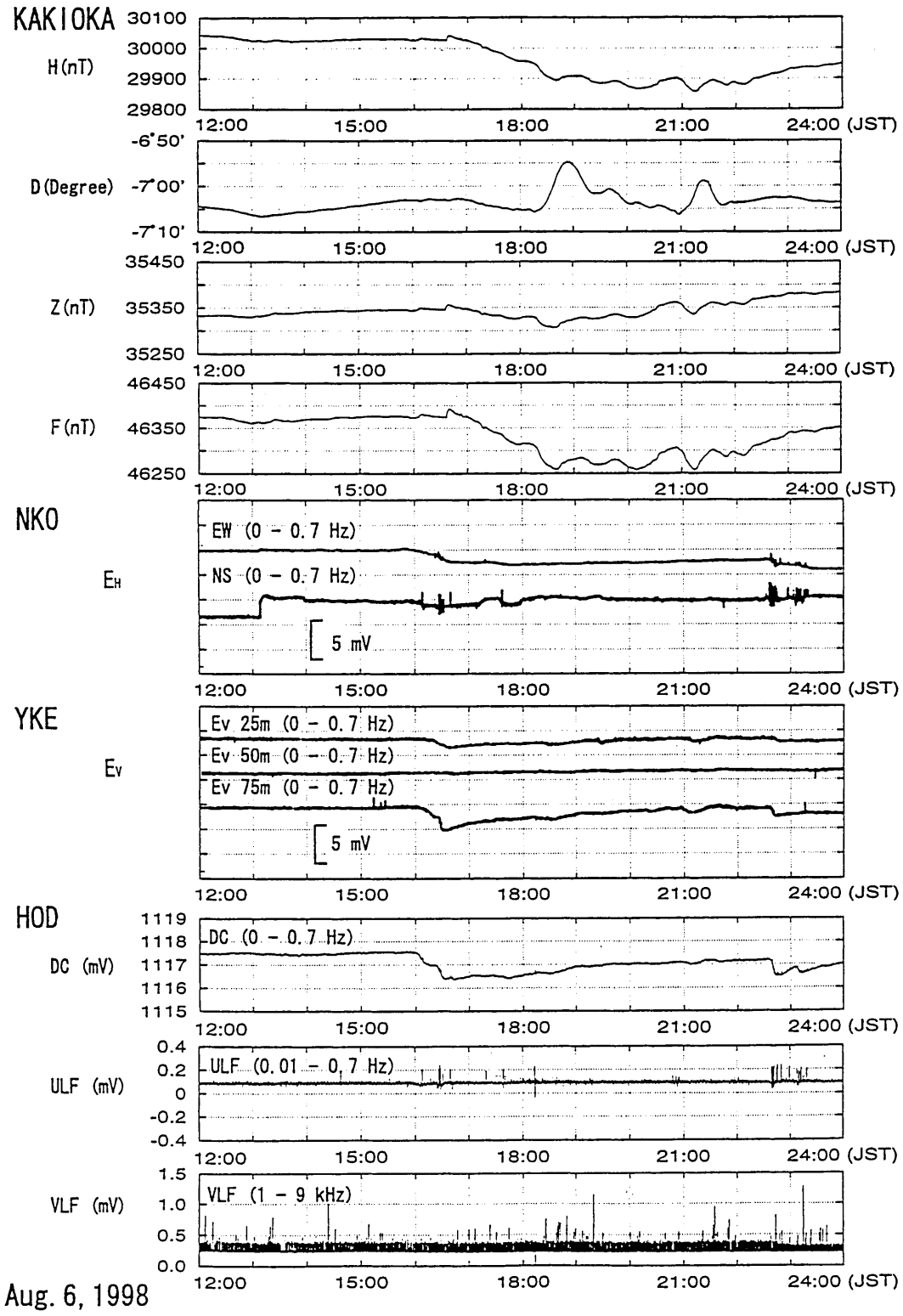

Fig. 4. Electric field recording data obtained by several measurement methods at the time of a severe geomagnetic disturbance. From top to bottom are shown three sets of geomagnetic data from Kakioka, induction telluric signals by horizontal dipoles at NKO and by vertical dipoles at three depths (YKE) (Nakayama *et al.*, 1999), and records in the three bands by the ULEM at Hodaka. The sites are shown in Fig. 5. The borehole antenna provides signals of the largest similarity with that of the longest dipole (YKE, Ev 75m).

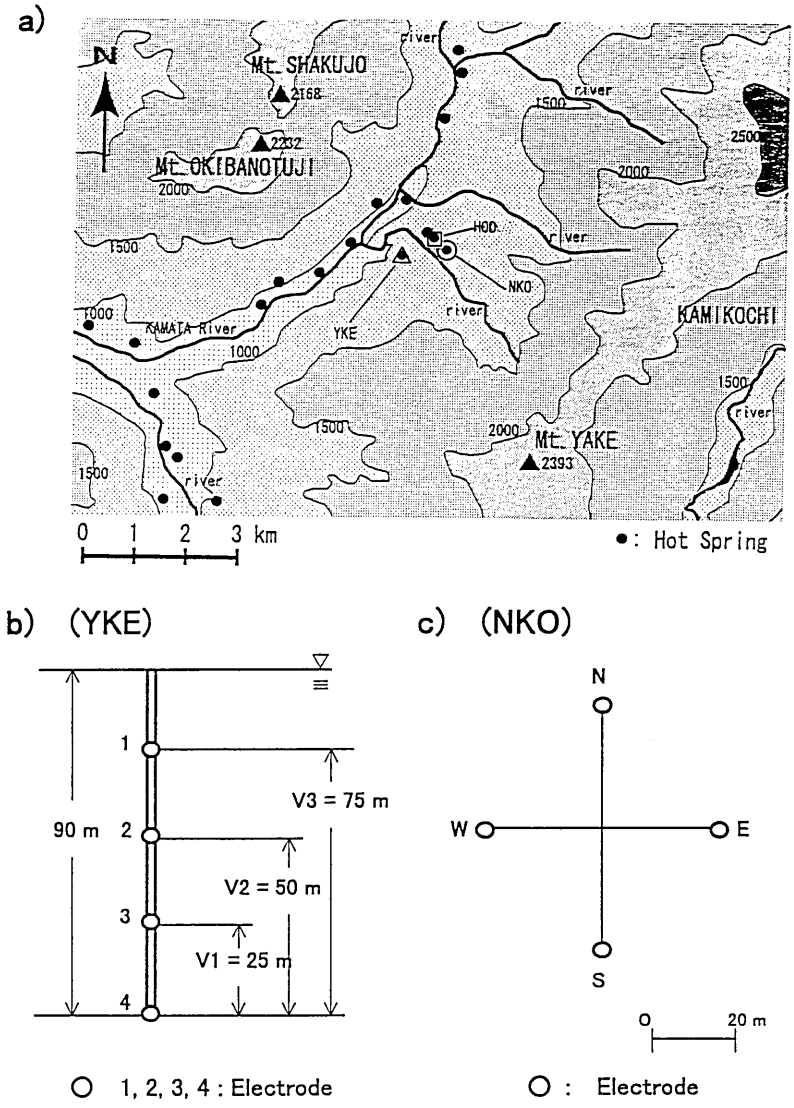

Fig. 5. Topographical map around the observation site Hodaka. a) Sites of electric potential measurement using three different methods are indicated as follows : ULEM (▣ HOD), horizontal dipoles (◉ NKO), and short vertical dipoles (▲ YKE). Hot springs are shown by ●. b) Arrangement of vertical dipole at YKE. c) Configuration of horizontal dipoles at NKO.

turbances induce only a small effect compared to field variations in relation to crustal activity. On the other hand, clear signals in association with the geomagnetic disturbances were recorded by the borehole antenna system, indicating that the sensor can detect induction electric signals by geomagnetic disturbances. Different electric field sensors of vertical dipoles and horizontal dipoles (Fig. 5) also recorded the disturbances. Records obtained by these independent instruments could be used to check whether or not the anomalies detected by our sensors are artifacts or result from malfunctions of the instruments (Fujinawa *et al.*, 2002 a).

Urban noise sources are situated on the ground surface, where conductivity is greatest, resulting in a concentration of electric current in shallower regions. There is large amplitude dissipation over the Earth's surface in a comparably conductive area such as in Japan. For example, a signal of 5 kHz dissipates $1/e$ at a depth of 70 m for a conductivity of 0.01 S/m. In addition, the vertical electric component E_z must be zero at the Earth's surface, because of the boundary conditions at the interface of conductive ground and the almost non-conductive atmosphere. Therefore, ULEM can be expected to obtain larger S/N for electric field variation measurements originating from crustal activity in the Earth.

Other noises are due to natural environmental

changes, such as atmospheric temperature, atmospheric pressure, and rainfall, which are usually large sources of noise in crustal deformation and chemical measurements (e.g. Rikitake, 1976 ; Park *et al.*, 1993). However, these changes were found to induce practically no significant effects in our measurements, at least within the limits of our recording parameters. This is one useful advantage of ULEM. Our explanation could be that electromagnetic noises induced by these phenomena are limited in shallower earth, inducing only a slight effect to our measurement system. A full monitoring record (Takahashi *et al.*, 2000) supplements the present description of noises from various sources. Thus, we need not pay much attention to these subsidiary data concerning environmental and civil noise when evaluating anomalies.

Therefore, our tentative criteria for detecting anomalies are background noise levels. This adopted criterion is a simple one, with the advantage stemming from the very small noises in these measurements. In terms of statistics, a more reasonable criterion should be determined through a probabilistic consideration (Fujinawa *et al.*, 1991) that is needed for an exact quantitative alarming. In addition, there is almost none of the elaborate data processing to depict meaningful anomalies that generally causes a loss of information (Wyss, 1991). Therefore, we do not consider these points unless specifically necessary.

3.2 Prominent Anomalies

A seismic swarm started on 7 August 1998 at the border between Nagano and Gifu Prefectures in central Japan (Fig. 6). The seismic parameters were determined using the extensive seismic network of NIED (Matsumura *et al.*, 1988). The observation site was very calm from 1993 to 1997 around the present seismic zone, compared to the current seismic activity (Fig. 7). Two exceptions were slight and spotted activity in July 1997 and low activity near Mt. Yake from July to December 1993, with the largest earthquake at a magnitude of 4.5.

The present activity took place at a distance of several kilometers from HOD site. The current swarm activity zone moved from north to south (Fig. 6). At the initial stage, from the start of the activity on 7 August until 11 August, the swarm was limited to the southern area near Mt. Yake, several kilometers east of HOD site. Meanwhile, the dominant activity moved to the northern region. It extended further north in early September to Mt. Noguchidake in Toyama Prefecture. The most active period was around the middle of August 1998, and it eventually ceased in December 1999 (Fig. 7).

The electric field records from typical days of the seismic swarm activity are shown in Fig. 8. We have previously shown the monitoring record that corresponds to the normal state on 5 August 1998, the day before the start of the swarm in the same recording range (Fig. 3). Fig. 8-1) shows the record on 7 August 1998 when the seismic swarm started. Fig. 8-2) depicts the record on 12 August, when the second-largest earthquake with a magnitude of 4.1 occurred, and Fig. 8-3) shows the record from 16 August, when the largest earthquake occurred, with a magnitude of 5.2. Electric field changes were anomalous on the day when the swarm started (Fig. 8-1), and more clearly anomalous on the days around the period of major earthquakes (Figs. 8-2) and 8-3)), compared to the normal state of almost flat record lines (Fig. 3).

A slight anomaly can be seen in the DC band (Fig. 8-1)), moderately clear variations in the ULF band, and a large variation anomaly in the VLF band from about 12 hours before the first earthquake (magnitude 3.9). Abrupt co-seismic electric field changes occurring at the exact time of the first earthquake are seen in the DC band, and on the ULF channel, but there are no conspicuous anomalies in the ELF/VLF band. The co-seismic changes in the DC and ULF bands are possibly induced by seismic ground movements in association with the arrival of waves (Nakayama *et al.*, 1997 ; Fujinawa and Takahashi, 1998 ; Nagao *et al.*, 2000).

Large, clear variations can be seen in the swarm on 12 August, when the second largest earthquake occurred (magnitude 4.1) (Fig. 8-2)). This earthquake marked the start of the second swarm activity, which extended to the north (Fig. 6). A slight level decrease with a longer period variation of about 8 mV appeared in the DC band at about 2 : 30 (JST) (B in Fig. 8-2)-(1)), eight hours before the earthquake, and a sharp decrease of 20 to 30 mV appeared at about 6 : 30 (C in Fig. 8-2)-(1)). Similar DC band changes were also seen to a small extent before the start of the swarm activity (A in Fig. 8-1)-(1)). Although there are occasionally very small-scale changes in normal states in the absence of any crustal activity, we had

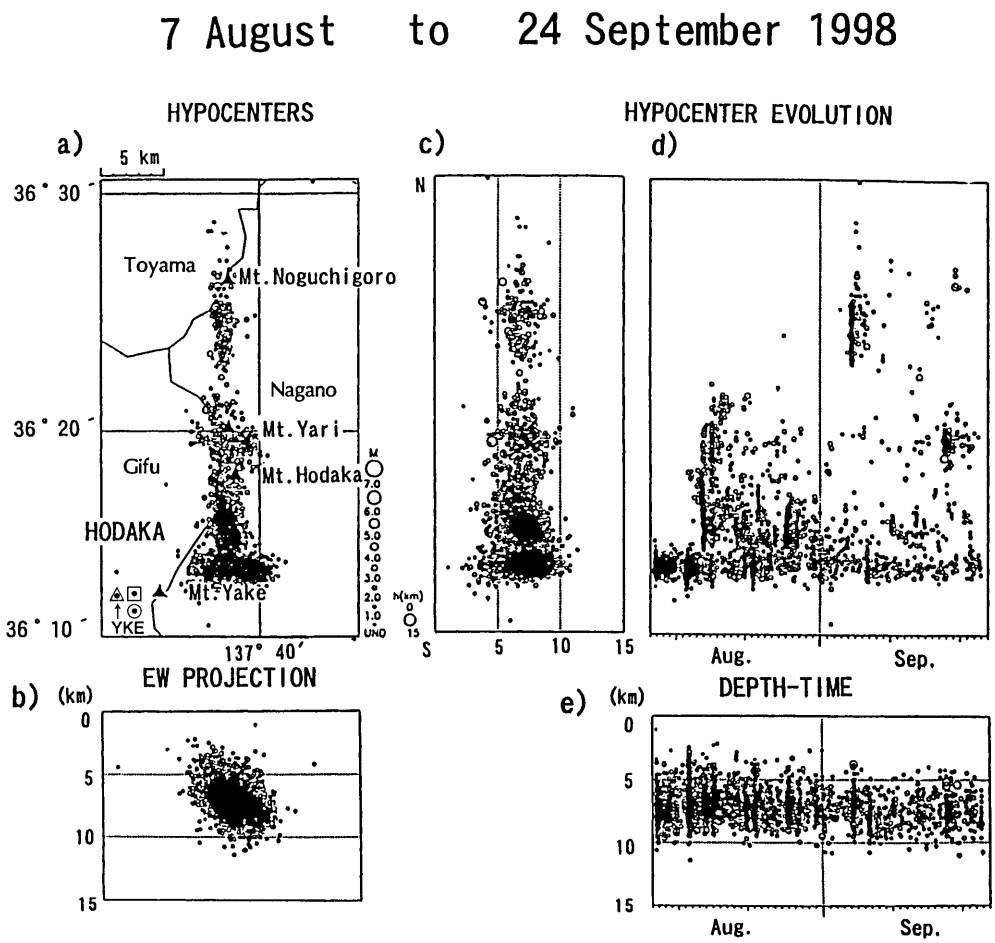

Fig. 6. A seismic swarm started on 7 August 1998 just west of the observation site at Hodaka (▣). The activity was practically the first since the observations started there in 1993 (Fig. 7). The hypocentral data (Japan Meteorological Agency ; (JMA)) indicate that the initial activity until 12 August was limited to east of Mt. Yake and extended northwards in the second stage of activity. Data from short vertical and horizontal dipoles maintained by Nagoya University about 600 m west of Hodaka site (◉) are utilized to supplement this research.

not seen observed such a large event as represented by "C" in Fig. 8-2)-(1) and "D" in Fig. 8-3)-(1). These trend-like changes start in a short time period and continue for half an hour to several days with strengths from several to several tens of mV. After a time interval, the DC levels return to near their previous levels.

There are many fluctuating component superposed on this large structure including ULF band variations. The ULF band monitoring record (in Figs. 8-2), 8-3)) shows much clearer anomalous variations than the DC component, mainly because of the tenfold amplification for the ULF band. Most dominant fluctuations in the ULF band are like "D" in Fig. 8-3). They are schematically represented in Fig. 9.

The typical ULF fluctuations shown in Fig. 9 are characterized by a sharp increase to a peak value *Ap* and a decrease to several tens of percent of the peak value, and a sharp decrease followed by a gradual decrease to a original. The peak value *Ap* is nearly uniform during a time interval from several hours to several days, probably corresponding to the steady state of the field generation mechanism during the lengthy time interval. The polarization of the change was unbalanced, in a dominantly negative sense in this case. However, in some time periods they were oppositely polarized (Fujinawa *et al.*, 1992 ; Takahashi *et al.*, 2000).

3.3 ELF/VLF Band

The ELF/VLF band suggests a different evolution than those of the other two bands. The ELF/VLF band signals appeared only at times of great strength in the other two bands, when seismic activity was substantial. An example from 12 August is shown in

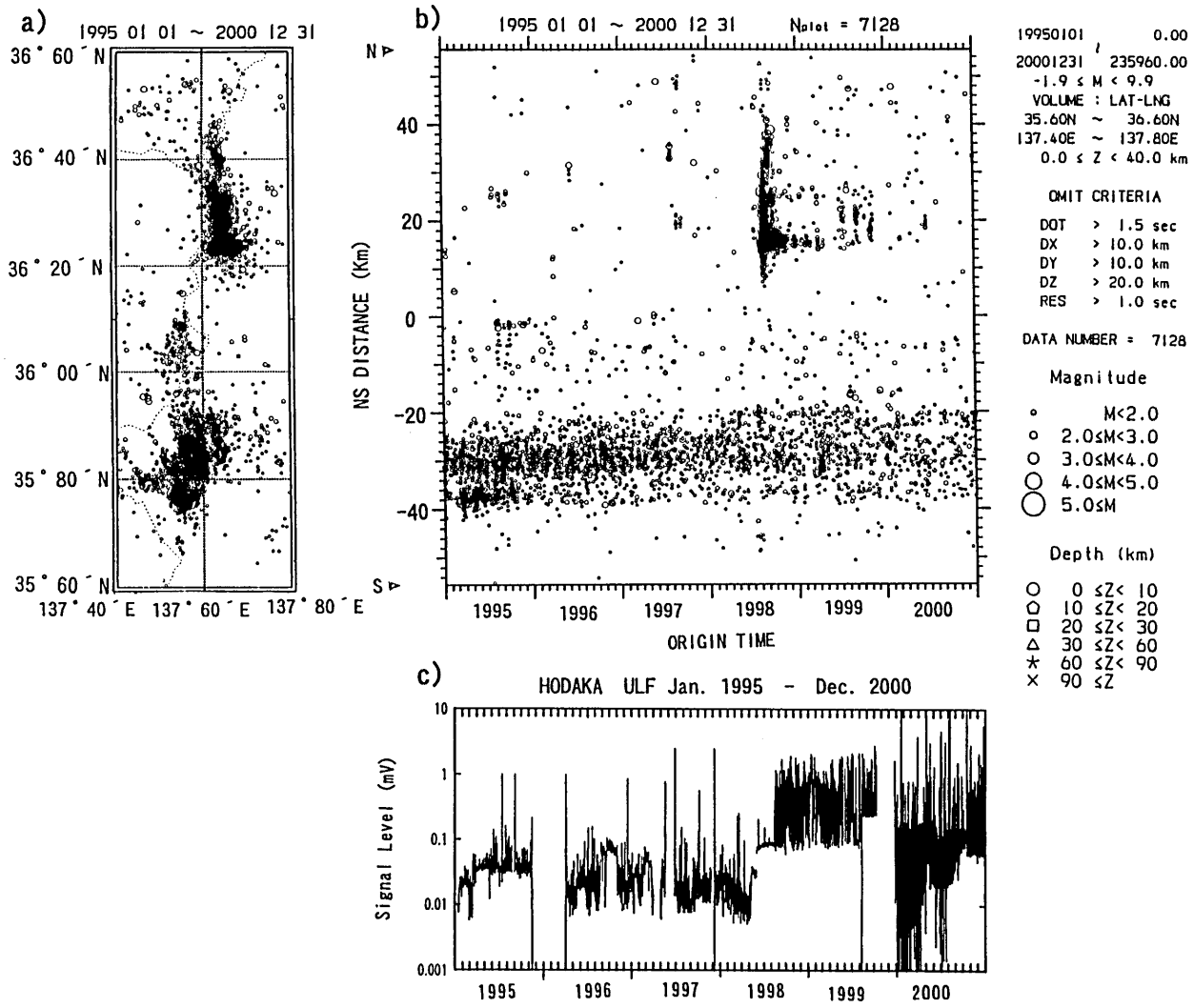

Fig. 7. Seismicity around the observation site determined by the Kanto Tokai Crustal Observation Network of NIED (Matsumura *et al.*, 1988). a) : Hypocenter distribution from 1 January 1993 through 30 December 1999 ; b) : Space-time distribution in the same period ; c) : The field strength record $U(t)$ for the ULF (Eq. 2). The anomalous variation that appeared from August 1998 was substantial, amounting to about 1 mV, in comparison with the background noise level of less than 0.1 mV. The anomaly had almost disappeared by December 1999, with an ordinary level of less than 0.1 mV. The variations at the time of vapor ejection in July 1996 did not appear in this form of representation, although they were discerned clearly in the original monitors (Takahashi *et al.*, 2000).

Fig. 8-2). This feature could be interpreted in terms of the frequency spectral characteristics of ground water movement that induce electromagnetic field generation as is described later in detail. Another aspect that differs from the other two lower frequency bands is that most of the signals observed in the normal state are atmospherics (Fujinawa *et al.*, 1997). Reduction of this kind of noise is underway and will be reported soon.

There were no reported severe lighting discharges around the observation site on 7 August 1998 (Franklin Japan, Inc.), although there was considerable rainfall around the Hodaka area (Japan Meteorological Agency : (JMA)). The time evolution of the electric field change (Fig. 8-1)) is similar to those at the times of lightning discharges (Takahashi *et al.*, 2000). However, the extremely long duration of the increases in the electric amplitude of the ELF/VLF band, such as that from 01 : 00 to 13 : 00 on 7 August (Fig. 8-1)), had rarely been seen since observations started in 1993.

It is suggested that there were precursory variation in this band. No pulse-like signals (VSP) were

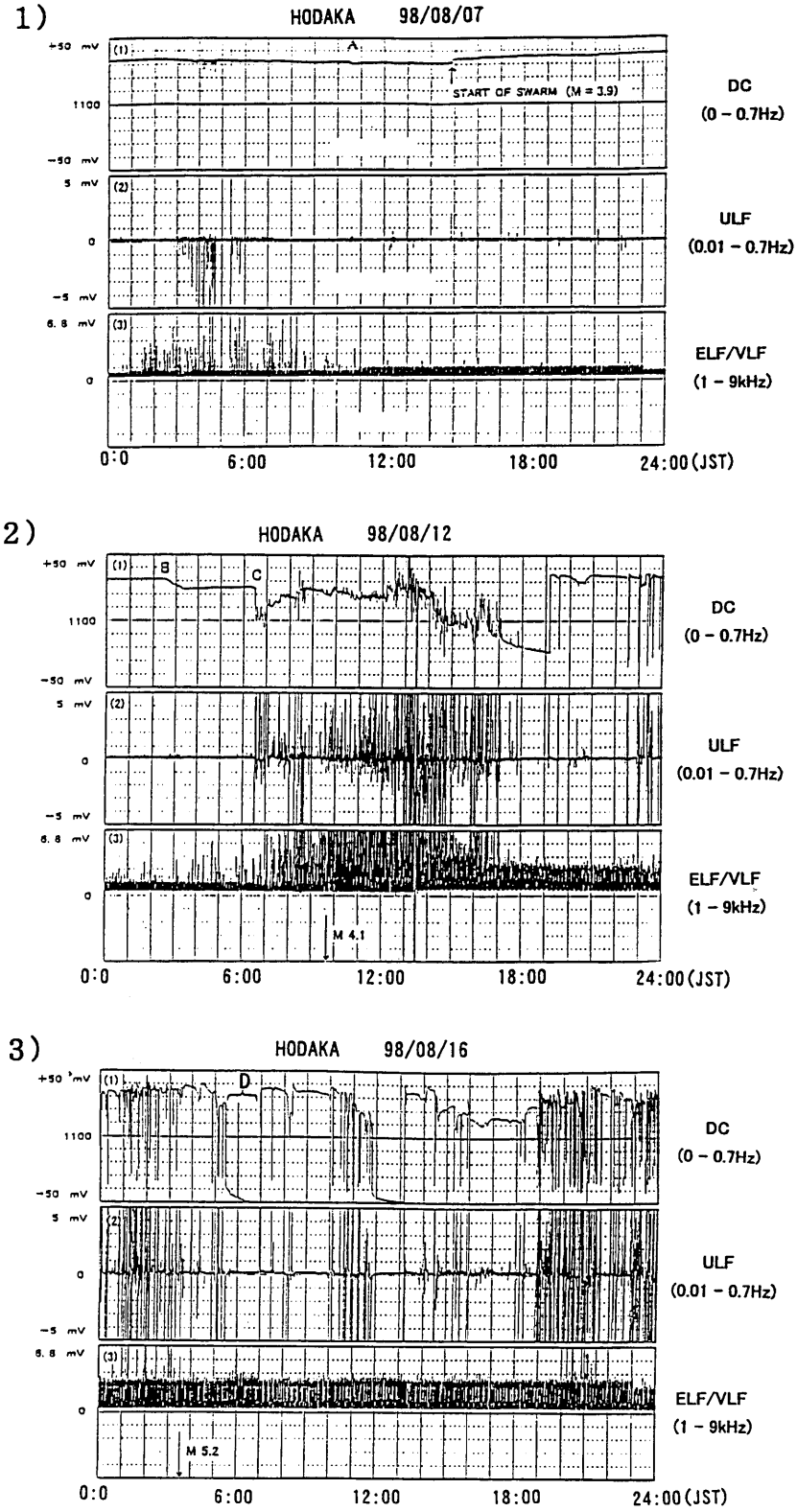

Fig. 8. 1) Monitoring records on 7 August 1998, when the swarm activity started at about 15 : 00. Anomalous transient electric field changes were observed in three frequency bands about ten hours before the first earthquake (magnitude 3.9). The starting time and the duration of the anomalous signals are somewhat different for the three frequency bands. 2) A very clear anomalous transient self-potential electric field change was recorded about seven hours before the occurrence of the second-largest earthquake (M 4.1) in the earthquake swarm on the DC channel (B) in 2)-(1). The earthquake marked the starting event of the seismic swarm in the second stage. About four hours after the appearance of the DC component anomaly, (C in 2)-(1)), ULF (2)-(2)), and ELF/VLF (2)-(3)) bands also recorded, almost simultaneously, large and clear anomalies. Urban noise in the ELF/VLF channel increased from about 0.8 mV to 2.4 mV during the period of the most active electric field anomaly occurrence. 3) Monitoring records on 16 August 1998, including the period when the largest earthquake (magnitude 5.2) occurred. Transient electric field anomalies dominantly consisted of a typical fluctuation, seen as -high-frequency pulse signals of negative polarity with a variable duration, from several seconds to several tens of minutes, as exemplified by D in 3)-(1). It is noted that they were accompanied only by minor anomalous signals in the ELF/VLF channel 3)-(3) in comparison with other channels.

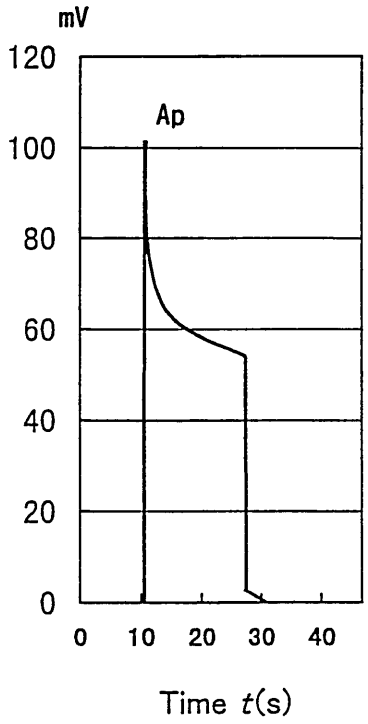

Fig. 9. A typical waveform is schematically shown for higher frequency electric anomalous signals at the time of a seismic swarm.

detected in the ELF/VLF band located around the seismic swarm region using the signal location determination method (Fujinawa *et al.*, 1997 ; 2001 a). This indicates that the ELF/VLF band variation in association with the seismic swarm was not as large as those due to the return strokes. VSP of the lightning stroke can usually be detected at other stations in the network, because of their substantial strength. We thus think that the present ELF/VLF emission is from the swarm region. It is also probable that the VLF signals were generated underground as will be shown later. Moreover, the source should be within a distance of about 1 km from the borehole sensor, because of the skin depth of several hundred meters.

The clearest ELF/VLF band anomalies were observed during the initial period of the second stage of the swarm activity, from about 07 : 00 to 17 : 00 (JST) on 12 August 1998. Similar duration and strength have not be seen in association with lightning return strokes (Takahashi *et al.*, 2000). Radiation of this large-scale amplitude and duration appeared on 12, 21, 22, 25, 26, and 28 August, when the swarm activity was strong and contained several earthquakes with magnitudes larger than 4.0. Sometimes there were indications of possible return strokes (Franklin Japan Co., Ltd.), but they were not as large as on other days when much smaller scale radiation than that shown in Fig. 8 was recorded. The waveform of the signals was not recorded at HOD.

3.4 Long-term Record

The degree of anomaly in the present case could be more clarified by examining all electric field data from the start of the observations in relation to crustal activity. All of the digitized observation data from 1995 to 1999 are available in printed form (Takahashi *et al.*, 2000). The strip-chart records prior to the digital recording could not be printed, but they do not contain any anomalies except for those kinds of noise discussed previously due to lightning discharges or noise at the time of calibration. Therefore, the anomalies at the time of the seismic swarm, such as illustrated in Figs. 8-2) and 8-3), can be attributed with confidence to crustal activity origins.

We present here a record that is limited in content and length because of the limited space available. Monitoring records for all of August 1998 (Fig. 10) illustrate how anomalous the present changes were after the start of the seismic swarm on 7 August. The ULF band variations are shown here in the same recording range as in Fig. 8. Large amplitudes that reach over-scaling are frequently seen from 12 August 1998, in contrast to almost a zero level before the start of the seismic swarm. Most records are flat in the normal state (Takahashi *et al.*, 2000). The apparent flattening that appears after the onset of large fluctuations is mainly due to electronic over-scaling, not to negligible variations or malfunctions.

It is difficult to present a long record in a condensed form without losing the detailed properties of the signal variations. To resolve this problem for the ULF signals $u(t)$, signal strength $U(t)$ is defined as

$$U(t)=\int_{t}^{t+T} | u | \, dt \qquad (2)$$

The value T is taken to be 60 s. The signal strength value for the whole period of the digitized recording is shown in the lower part of Fig. 7 (c). A spatio-temporal representation of seismicity is also shown here (Figs. 7 a, b). We can see that the signal level increased by about one order compared to the normal level at the onset in the second stage of the seismic swarm. A substantial level was maintained during seismic activity until early April 1999, and

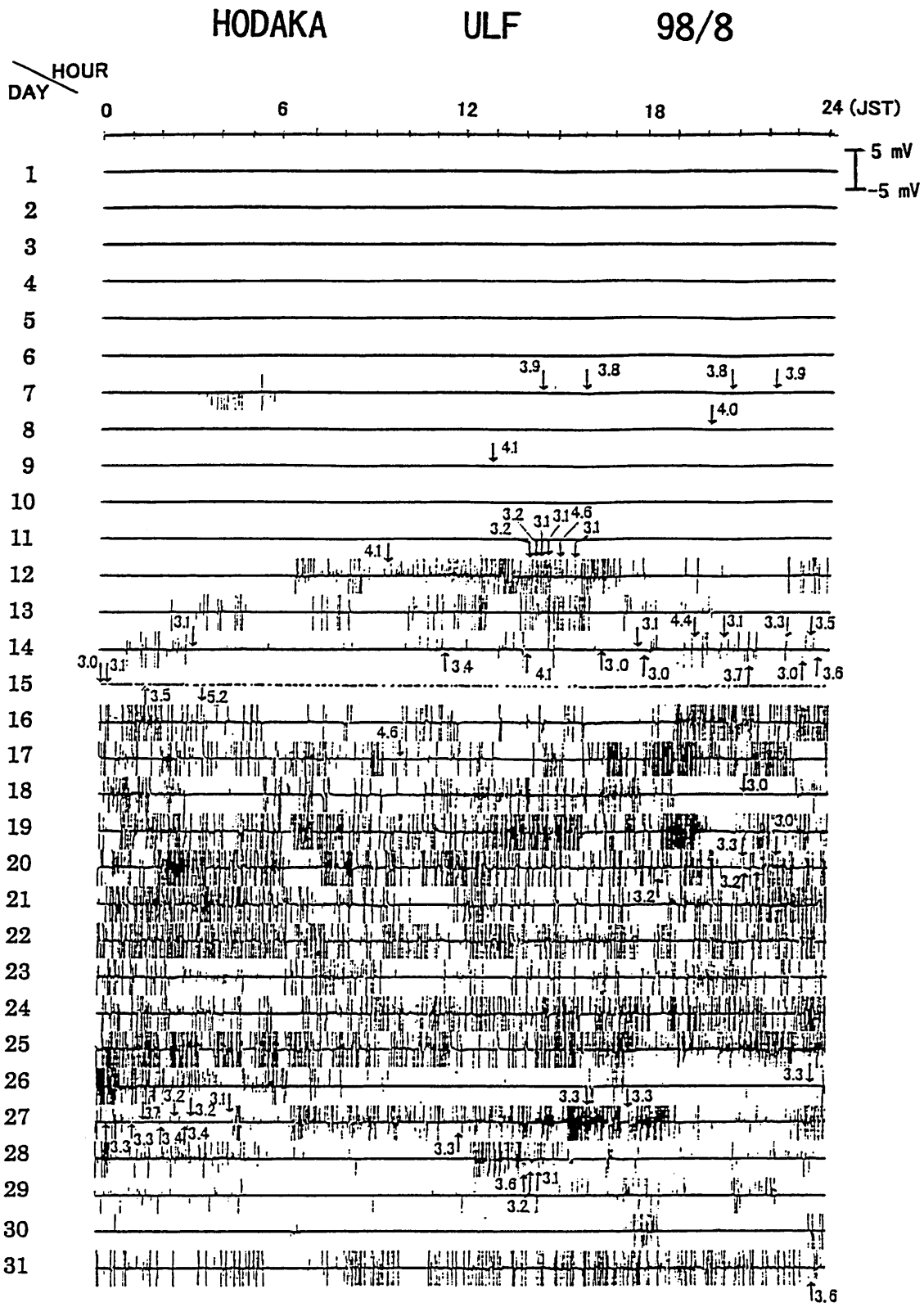

Fig. 10. Monitoring records for the ULF channel for the whole of August 1998, including the normal stage until 6 August and the anomalous stage associated with the seismic swarm that started on 7 August. Data was lost on 15. Earthquakes with a magnitude larger than 3.0 are indicated by arrows in the waveform trace. Correlations of individual earthquakes with transient electric field anomalies are not clear because of the high frequency of earthquakes that occurred in a swarm activity, except for some special earthquakes occurring around the starting times of different stages of seismic activity.

then decreased to the original level of 0.01 mV at the end of 1999, well after the actual cessation of the swarm. However, the small increase of the level in the initial stage can scarcely be seen in this representation, although we can discern it in the enlarged record shown in Fig. 8-1), which was previously explained in detail. More suitable parameter than that of Eq. (2) are needed.

Electric field stength well correspounds in time to the crustal activities. Looking backward from the start of the swarm, we can see there is a sharp increase of a half order around 8 May from about 0.01 mV. We can assume that there were medium-term precursors to the present swarm about three months before the event. And the level 0.01 mV is tentatively taken to be the background signal level. A statistical analysis of the signal level and crustal activity for a sufficiently long observation period containing a large number of crustal events can provide us with a plausible criterion for anomalies to discriminate from the normal state (Utsu 1983 ; Fujinawa, 1991). Our conclusion is not well confirmed from this viewpoint, because sufficient events were not included in the test data.

3.5 Correlation with Particular Earthquakes in the Swarm

The anomalous electric field changes at the time of the largest and the second-largest earthquakes were very large as seen in Figs. 8-2) and 8-3), and it is possible to attribute these anomalies to particular earthquakes. We could not recover the digitized data on the day before the largest earthquake, 15 August. But we know from the strip chart record that the largest fluctuations preceded this earthquake. It is indicated that the earthquake was preceded by a very large electric field variation, which caused overscaling (Takahashi *et al.*, 2000).

However, it is hard to make anomalies in the smaller earthquakes correspond to a particular earthquake, because of the persistent appearance of large electrical variations and occurrences of consecutive earthquakes (Fig. 7). Moreover, very large electric field variations in October 1998 accompanied only smaller earthquakes with magnitudes of less than 3.5 (Fig. 7). A comparison of signal levels and swarm activity leads to the conclusion that it is not possible to correlate large anomalies with large-scale earthquakes, except in the earlier stages of seismic activity.

There were several activities around the area of the present seismic activity in 1993, 1995, 1996, and 1997 (Figs. 7 a and 7 b), accompanied by anomalies of a much smaller strength (Takahashi *et al*, 2000). One example is a small vapor eruption around the observation site (Nakayama *et al.*, 1997). Fluctuations in the ULF band of ± 2.5 mV amplitude appeared for about two months. The anomalies consisted of some tens of pulse-like signals per day, providing a very small value of U, and thus are not seen in the reduced recording shown in Fig. 7 c. Electric field variations were much smaller both in strength and duration compared to the present cases. A comparison of Figs. 7 b and 7 c indicates that the electric field variation is very small when there is no crustal activity.

We can conclude that the anomalous electric field changes at HOD in 1998 were related to the earthquake swarm occurrence and were not induced by other extraneous natural phenomena, such as geomagnetic disturbances, atmospheric disturbances including lightning, or urban noise. The phenomena can be utilized in a forecast algorithm with a sufficiently small probability of errors.

4. Discussion

4.1 Detection Selectivity

The seismic activity in the electric field observation period around the observation sites exhibits a heterogeneous distribution. First, we discuss the signal detection difference for a larger scale based on seismic activity data around the observation site.

In addition to the present activity, there was conspicuous seismic activity about 50 km south during the observation period (Fig. 7). However, scarcely any anomalous signals were detected at HOD in association with this activity. And no other sites in our observation network (Fig. 1) detected any anomalies in accordance with the present swarm activity. Detectability is less than several tens of kilometers for ULF band variations in the geological structures in and around the network. The signal detectability is limited within a distance of several times the spatial dimensions of the seismic activity, in agreement with the electromagnetic measurements (Bernard and Le Mouel, 1996) as well as groundwater anomalies (e.g. Scholtz, 1990).

Next, we discuss detection heterogeneity on a

much smaller scale. The first stage of the seismic activity from 7 August 1998 that occurred in the southern part of the swarm area (Fig. 6) gave rise to only small variations at HOD, compared to the much larger ones in the second stage, which started on 12 August. The hypocenters in the first stage were limited to the small southern area. There is a clear boundary of detectability of anomalous signals at HOD for the seismic zone, divided into the earlier active zone and the later main active zone. The two zones are very near each other, separated by an aseismic zone only about 1 km wide, and the southern zone is nearer to the observation site than the second main zone. A high-resolution image of the hypocenter determination (Yoshida *et al.*, 1998) indicates that the border corresponds to the geological boundary (Takahashi *et al.*, 2000). We can suspect that there is a much better physical connection between the site at HOD and the northern region of the second seismic activity in terms of electric signal observation.

This kind of heterogeneous detectability of electric signals has been presented to discuss the signal propagation characteristics of the Seismic Electromagnetic Signal (SES) asserted in Greece (Varotsos and Lazaridou, 1991 ; Varotsos *et al.*, 1996 ; Surkov *et al.*, 2001). Detectability heterogeneity has been explained by the presence of a conductive path between the observation site and the signal source, taking into account the frequency dependence of signal dissipation. However, based on the present findings and results of estimations using a streaming potential model (Fujinawa *et al.*, 2002a), we are inclined to believe that the heterogeneity can be primarily attributed to the heterogeneity of the source generation zone. In addition, the signal dissipation difference in the resistive and conductive layers is favorable for a substantial electric potential difference, with the result that the ULEM can effectively detect even slight variations. ULEM is expected to have greater potential for detecting anomalies because of the shorter distance to the generation zone.

A different type of vertical electric field observation was conducted at the NKO site, about 400 m west of the Hodaka site (Nakayama *et al.*, 1997). They used three pairs of vertical electrodes of 25 m, 50 m, and 75 m, with an electrode at the bottom of the borehole acting as a common ground. Additionally, two horizontal and mutually perpendicular dipoles 50 m long (Fig. 5) were installed earlier than the borehole sensor. Comparing the observational data from these sites with data from ours provides a valuable clue for determining the source location of anomalous electric field changes. The electric strength drop B on 12 August (Fig. 8-2)), detected by different sensors of the vertical electric field at HOD and YKE, indicates that the vertical gradient of the electric field strength was predominantly concentrated in a region at a depth of more than 75 m. The same holds true for the typical ULF anomalous signals shown in the record section from 19 : 10 through 24 : 00 (Fig. 8-3)). These pulse-like signals rarely appeared on the shallower electrodes or in the horizontal dipoles, suggesting that their origins lie deep underground.

Therefore, we assume that the source region of the present electric anomalies is at least 100 m deep. High-frequency components dissipate faster than low-frequency components. We will show later that high-frequency ULF signals are generated at a short distance of several kilometers under the usual conductivity value of 100 Ω-m. Therefore, we can infer that the source of the present anomalies is around Mt. Yake, and that the HOD site has a good electromagnetic connection with the hydrothermal circulation network in the northern part, which induces seismicity in the first stage, but not with that in the southern zone. A hydro-dynamic connection at HOD is not probable because of the negligible temperature perturbation in this well during the present seismic swarm.

Present finding is important from the standpoint of the detection method for small electromagnetic signals with a high rate of dissipation, as well as slight ground water movement under conditions of high heterogeneity. Installing the sensor near the source, such as using a casing pipe, seems to be highly advantageous. For example, the ELF/VLF signals decay very rapidly for an electrical resistivity of 100 Ω-m of the skin depth of several tens of meters. Even small signals (Fig. 8-(3)) could have been detected using a casing pipe antenna, because of contact with or proximity to the source of the electric field generation, such as a confined water layer.

The long antenna has advantages and disadvantages. One advantage is substantial detection poten-

tial without any detailed knowledge of the confined water layer or conductivity distribution, because of its contact with many layers where electromagnetic signals are propagated at different dissipation rates. In addition, an electric field measurement is more practical than a magnetic measurement due to the easier installation of the sensor. A disadvantage is that we cannot accurately determine where the sources are, because there is no information about the vertical location. However, every measurement, including dipole measurements, requires the conductivity distribution to locate the source. Therefore, this disadvantage is not a serious defect of the ULEM, at least not in this stage of the investigation of confined water movement and detection of precursory electric field anomalies.

5. Generation Mechanism

Present analyses provide plausible evidence that electric field anomalies exist in association with a seismic swarm. It is also suggested that the source region lies deep underground. Our observations at 12 sites in central Japan, ongoing for more than ten years from 1989, suggest that all sites in and around the geothermal region (Awano, Izu-Oshima, Miyakejima, Ito-Motomachi, and Hodaka) lead to the same conclusion as at HOD ; anomalous electric fields are detected only at the time of seismic swarm or volcanic eruption (Fujinawa and Takahashi, 1990 ; Fujinawa *et al,* 1992 ; Fujinawa *et al.,* 2000 ; 2002 a). The other sites have not recorded similar anomalies, and there have been no seismic swarms and no volcanic eruptions around the sites.

In addition to our results, several field observations indicate that electric field anomalies in the ULF band can be found in the geothermal zones (e.g. Zlotmicki and Le Mouel, 1990 ; Bernard, 1992). High-temperature water circulation is common in the geothermal region (e.g. Ingebritsen and Sanford, 1998). It is thus natural to assume that confined water plays some role in the process of seismic and volcanic activities.

We presented that the anomalous ULF band signals observed at the time of a seismic swarm are dominated by typical pulse-like signals, as shown schematically in Fig. 9. Similar anomalies were also detected in association with crustal activities at five sites situated in a geothermal area. We detected this kind of variation at Izu-Oshima Island, while an almost periodic seismic swarm occurred east of the Izu peninsula (Fig. 11 a ; Matsumoto *et al.,* 1996). Similar anomalies were detected at the Awano siste during a recent seismic swarm that occurred about 20 km northwest of the site (Fig. 11b ; Fujinawa *et al.,* 2002a), at Izu-Oshima at the time of a small volcanic eruption in 1990 (Fig. 11 c ; Fujinawa *et al.,* 1992), and at Miyakejima Island at the time of a volcanic eruption (Fig. 11 d ; Fujinawa *et al.,* 2001 b). These electric signals were all obtained using the ULEM.

Electromagnetic field variations as self-potential changes have been attributed to piezo-effects, MHD effects, and electro-kinetic effects (Nourbehecht, 1963; Fenoglio *et al.,* 1995). A quantitative comparison of these effects has demonstrated that electro-kinetic effects are about one-order greater than the other effects. We accept these results, although there may be situations in which these effects dominate in regimes that were not taken into account in the evaluation. The typical electric field variation is, therefore, assumed to be a transient part of the self-potential (TSP). Here, we present a quantitative discussion on the typical variation to investigate the signal source.

Mizutani *et al.* (1976) were the first to attempt to explain the magnetic anomalies associated with the Matsushiro seismic swarm based on electro-kinetic effects. The self-potential (SP) anomaly has been interpreted by a generation mechanism better founded (Ishido, 1999 ; Ishido and Mizutani, 1981 ; Murakami, 1989 ; Yoshida *et al.,* 1997) than other electromagnetic phenomena (e.g. Park *et al.,* 1993 ; Parrot *et al.,* 1993).

Electromagnetic fields can be generated by ion transport in fluids through electro-kinetic effects by means of the interaction between fluid motion and electric currents. The coupling is described using the relation :

$$\begin{pmatrix} \boldsymbol{I}_e \\ \\ \boldsymbol{I}_f \end{pmatrix} = \begin{pmatrix} L_{11} & L_{12} \\ \\ L_{21} & L_{22} \end{pmatrix} \begin{pmatrix} -\nabla\phi \\ \\ -\nabla P \end{pmatrix} \qquad (3)$$

where $\boldsymbol{I}_e$ is the electric current density, $\boldsymbol{I}_f$ the fluid volume velocity, ϕ the electric potential, P the pore pressure, and L_{ij} the generalized coefficients of conductivity (Overbeek, 1953 ; Nourbehecht, 1963 ;

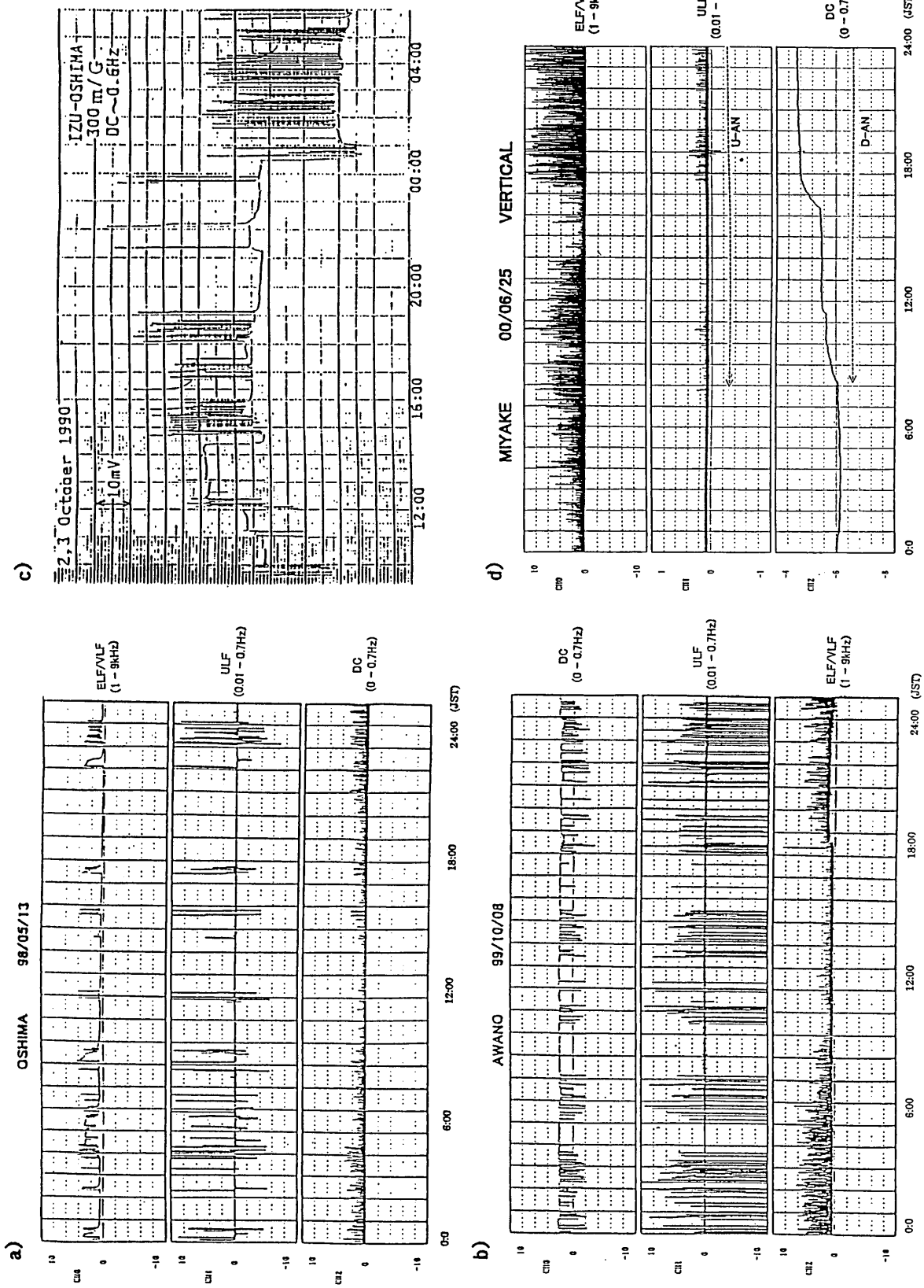

Fig. 11. Electric field anomalies assumed to be related to earthquakes. Two of the cases are for seismic swarms observed by the ULEM at (a) Izu-Oshima and (b) Awano. The other two cases are volcanic eruptions at (c) Izu-Oshima and at (d) Miyake-Jima.

Mizutani *et al.*, 1976). L_{11} is the electrical conductivity and L_{22} the fluid permeability in Darcy's law. The cross-coupling term containing L_{12} or L_{21} corresponds to the electro-kinetic effect with L_{12}/L_{11} as the streaming potential coefficient ($=C$) and L_{21}/L_{22} the electro-osmosis coefficient.

From Eq. (3), the electric current density $\boldsymbol{I}_e$ is described as

$$\boldsymbol{I}_e=-\sigma(\nabla\phi+C\nabla P) \tag{4}$$

and the streaming potential coefficient as

$$C=\varepsilon\zeta/\sigma\mu_f \tag{5}$$

where ζ is the zeta potential in an electric double layer formed at a solid-liquid interface, ε the dielectric constant of the fluid, σ the electric conductivity, and μ_f the viscosity of the fluid. This type of formulation has been adopted to explain the anomalous electromagnetic field changes when an earthquake occurs (Mizutani *et al.*, 1976 ; Murakami 1989 ; Dobrovolsky *et al.*, 1989 ; Fenoglio *et al.*, 1995) and the self-potential distribution in geothermal fields (Ishido and Pritchett, 1999).

Previous descriptions of an electromagnetic field resulting from the electro-kinetic effect have been limited to stationary cases, and the source region is assumed to be at the boundaries of different substances (e.g. Fittermann, 1978). An extended estimation of the induced field in the case of transient generating forces was first attempted by Majaeva *et al.* (1997). A reformulation has been provided in the form necessary to analyze the waveform of anomalous variations (Fuinawa *et al.*, 2002 a). In the following, we briefly describe the formulation.

A more general formulation is based on Maxwell's equations for unsteady electromagnetic fields. Assuming a quasi-stationary situation with negligible displacement current in the ordinary crustal conductive medium of a piece-wise continuous continuity, Maxwell's equations are :

$$\nabla\times\boldsymbol{E}+\frac{\partial\boldsymbol{B}}{\partial t}=0 \tag{6 a}$$

$$\nabla\times\boldsymbol{H}=\boldsymbol{I}^{(t)} \tag{6 b}$$

$$\nabla\cdot\boldsymbol{B}=0 \tag{6 c}$$

$$\nabla\cdot\boldsymbol{E}=0 \tag{6 d}$$

where $\boldsymbol{E}$ is the electric field intensity, $\boldsymbol{B}$ the magnetic induction, $\boldsymbol{H}$ the magnetic field intensity, and $\boldsymbol{I}^{(t)}$ the total electric current. Under the assumption of a negligible electro-osmetric effect, the total electric current can be broken down into :

$$\boldsymbol{I}^{(t)}=\boldsymbol{I}+\boldsymbol{I}^{ext} \tag{7}$$

where $\boldsymbol{I}$ is the internal current relating to the electric field intensity through a constitutive relation and $\boldsymbol{I}^{ext}$ is the external current generated in non-electromagnetic processes (e.g. Rokityansky, 1982), a component induced in this case by the electro-kinetic effect through the pore water pressure gradient.

In addition, we use the constitutive equations ;

$$\boldsymbol{D}=\varepsilon\boldsymbol{E}, \tag{8 a}$$

$$\boldsymbol{B}=\mu\boldsymbol{H}, \tag{8 b}$$

$$\boldsymbol{I}=\sigma\boldsymbol{E} \tag{8 c}$$

where μ is the magnetic permeability. The external electric current $\boldsymbol{I}^{ext}$ can be naturally derived from Eq. (4), Eq. (5), and Eq. (6) as

$$\boldsymbol{I}^{ext}=-\sigma C\nabla P \tag{9}$$

The electromagnetic field in a piece-wise continuous medium can be described by the following partial differential equations, containing a unique electromagnetic field quantity of interest :

$$\left(\triangle-\frac{1}{\kappa^2}\frac{\partial}{\partial t}\right)\boldsymbol{F}=-\boldsymbol{\rho}(\mathbf{r},t) \tag{10}$$

$$\frac{1}{\kappa^2}=\sigma\mu$$

where $\boldsymbol{\rho}$ is the forcing term for the specified field quantity of interest $\boldsymbol{F}$: electric field intensity $\boldsymbol{E}$, magnetic field intensity $\boldsymbol{H}$, and vector potential $\boldsymbol{A}$ ($\boldsymbol{H}=\nabla\times\boldsymbol{A}$). The forcing terms $\boldsymbol{\rho}$ are,

$$\boldsymbol{F}=\boldsymbol{E}\ ;\ \boldsymbol{\rho}_E=-\mu\partial\boldsymbol{I}^{ext}/\partial t \tag{11 a}$$

$$\boldsymbol{H}\ ;\ \boldsymbol{\rho}_H=\nabla\times\boldsymbol{I}^{ext} \tag{11 b}$$

$$A\ ;\ \rho_A=\mu I^{ext} \qquad (11\,c)$$

if boundary conditions on the surrounding surface of S for domain V and the initial condition are specified for the solution of Eq. 10. Green's function in the frequency domain can be obtained by procedures of Raiche (1974) and Weidelt (1975) for layered earth.

We can calculate the transient electric field if the pressure distributions are given in a specified conductivity distribution. Here, we assume the simplest conductivity distribution of a uniform space for simplicity. We infer the pressure distribution, which provides the observed electric field. We assume that the pressure distribution is a product of the spatial part and the temporal part. The spatial distribution is further assumed to be uniform in a cubic region. We obtain the source time function of the perturbed pressure change by means of the forward method to find plausible pressure changes by trial and error.

The result is illustrated in Fig. 12. We attempted to match the observed signal ("ob." in Fig. 12) with the calculated signal ("cal.") by adjusting the rate of pressure change $\partial P/\partial t$ ("sou."). The calculated field is at a distance $r=300$ m by assuming the conductivity $\sigma=0.01$ S/m. The obtained synthetic waveform that corresponds to the assumed forcing term is shown in Fig. 12 (cal.). There is a satisfactory degree of similarity between the waveform of the source function and the synthetic curve. We could easily reduce minor discrepancies in the synthetic waveform by choosing a more appropriate function. In principle, we can infer the source time function from the observed signals at several points if we have sufficient knowledge of the streaming potential coefficient and conductive distribution.

The pressure change exhibites a rapid increase (phase 1), maintains the peak value for a short time (phase 2), decreases rapidly to about half of the peak value (phase 3), decreases very gradually over a long time (phase 4), and finally decreases to near zero (phase 5). The rapid increase might correspond to a rupture of the sealed compartment (Byerlee, 1993 ; Fenoglio *et al.*, 1995). Fenoglio *et al.* (1995) assumed that the rupture generates seismicity.

The strength cannot be obtained separately for the spatial and temporal parts of the pressure change in the inversion. Here, we rely on the discussion of Fenoglio *et al.* (1995) to discuss the temporal change

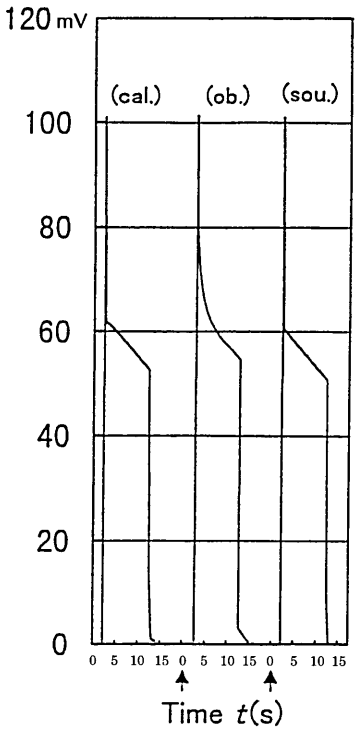

Fig. 12. A comparison of the synthetic waveform (cal.) for the source function (sou.) and the observed waveform (ob.). Scale of Vertical axes for synthetic and observed wave form. Scale of Vertical axes is for synthetic and observed waveform.

part. The inverted value of the source parameter is

$$\text{Source Volume}: Vs=26\,\text{m}\times 26\,\text{m}\times 26\,\text{m} \qquad (14)$$

which we assumed as,

$$|\nabla(\partial P/\partial t)| \sim 4\,\text{MPa/m}\cdot\text{s}$$

$$\zeta=0.1\,\text{V (Ishido and Mizutani, 1981)}$$

$$\varepsilon=8\varepsilon_0$$

$$\sigma=0.01\,\text{S/m}$$

$$L_{22}=10^{-11}\,\text{m}^2\text{(Brace, 1980)} \qquad (15)$$

The spatial pressure difference $\triangle P$ in the high compartments compared to the surrounding rock is

$$|\triangle P| \sim 170\,\text{Mpa} \qquad (16)$$

about 2% of the lithospheric pressure at a 4 km depth. The value is within a reasonable range (Fenoglio *et al.*, 1995). The fluid velocity in the fractured compartment is

$$|I_t| \sim 4\times10^{-3}\,\mathrm{cm/s} \qquad (17)$$

The electric field changes at several distances from the source are shown in Fig. 13 for the estimated pressure change. The calculations are for three cases of conductivity : σ=0.001 S/m, 0.01 S/m, and 0.1 S/m. The time evolution of the electric field E is similar at the zone near the source because of the diffusion property; i.e., phase 1 and phase 2 with a sharp change are conserved in the near field (Fig. 12). However, the signal is sufficiently diffused several kilometers from the source to lose the original sharpness. The degree of signal deformation increases with the distance from the source, and the amplitude decreases very rapidly. The signal waveform roughly reveals the source distance. We can presume that the typical anomalies containing a sharp rise were generated near the observation point. The amplitude ratio of the main phase 4 to the peak value was also conserved in the near field, but decreased rapidly in the far field. This property could also be used to infer the source distance.

6. Discussion

Most of the items in the evaluation guidelines (Wyss, 1991) were taken into account in the course of presenting evidence to demonstrate that electric field anomalies accompany earthquakes. We will now discuss the items not previously mentioned.

It seems natural to expect that the largest electromagnetic variations occur at the instant an earthquake occurs if the particular phenomena are precursory changes. We reported that a large associated field strength was observed for large-scale crustal activity in the time range of days. However, we could not associate the large signals with large earthquakes in a short time window of several seconds. We could interpret this aspect from the generation mechanism described previously. The electric field variations are not directly attributable to the mechanical earthquake rupture process, but through confined water movement. Experimental evidence suggests that there is time delay between the mechanical rupture and ground water motion. The water movement might be almost finished at the time of the main rupture, resulting in no co-seismic conspicuous electric variation. Therefore, this item in the requirements of the IASPEI guidelines should be modified, considering the possibility of precursors not directly induced in the mechanical rupture of faults, such as thermo-hydro dynamic changes in the groundwater circulation due to magma approach, which could be involved in the generation of electric field changes (Fujinawa *et al.*, 2001 b).

Another point concerns the field strength proportional to the epicentral distance. Our result that detectability is limited to the site nearest the crustal activity zone is in agreement with this item of the guidelines. However, we demonstrate that there are strong heterogeneities due to the variable hydrodynamic and electromagnetic connectivity. In these situations, we cannot expect a simple proportional relation between the field strength and the epicentral distance. Therefore, a modification should be considered that takes into account the heterogeneous property of the crustal medium where precursory events are occurring.

The third point regards the ratio of the danger zone size to that of the total monitored region. We could not provide an exact size ratio because of the very limited number of existing sites. The monitoring zone could not be quantified properly, because of the sparse distribution of sites and the heterogeneous detectability. However, the present method would not require very large zones or very many monitoring sites if we use the wells for fluid utilization, such as water, oil, and vapor pumping. These wells could have better hydrodynamical and electromagnetic connection to areas of crustal activities.

We limit this article to seismic swarms and volcanic eruptions. Earthquakes of both main-shock and aftershock types have occasionally provided anomalous ULF variations in our measurement, but to a much smaller extent. It is probably because of the much more restricted distribution of perturbed ground water circulation around the faults. Electric field anomalies were also reported in the main-shock and aftershock earthquakes in California (Fraser-Smith *et al.*, 1990) and in Taiwan (Liu *et al.*, 2000). It is interesting to note that the latter case, at the time of the disastrous Ji-Ji earthquake, showed a diurnal strength variation in the geomagnetic field (Yuan *et al.*, 2000, Private Communications), similar to the magma activity at Miyakejima Island and Izu-Oshima Island (Fujinawa *et al.*, 2001 b), with the similar preceding time period. It is suggested that the

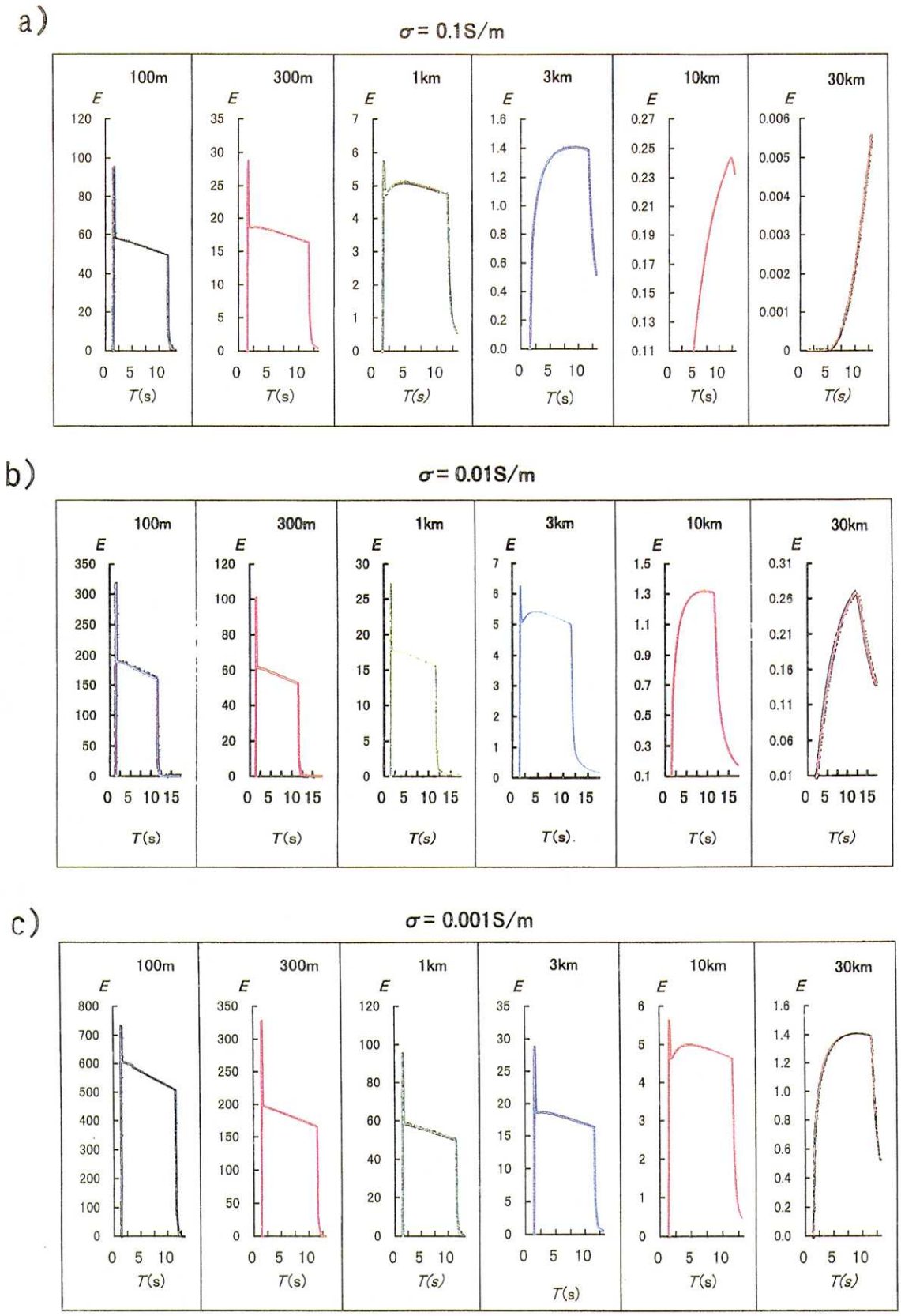

Fig. 13. Electric field variations at several distances from the source for the inverted confined pressure changes ("sou" in Fig. 12) for three cases of conductivity : a) σ=0.001 S/m ; b) σ=0.01 S/m ; and, c) σ=0.1 S/m.

anomalies are closely related to confined water.

Ground water plays an important role in mainshock and aftershock types of earthquake (e.g. Hickman *et al.*, 1995). There are numerous reports of groundwater anomalies preceding those kinds of earthquake (e.g. Rikitake, 1976 ; Wakita *et al.*, 1987) induding a report dealing with a concentrated water content around the fault (Zhao and Negishi, 1998 ; Fujinawa *et al.*, 1999). We could expect to detect significant preceding anomalies if we had suitable number of ULEM around faults.

Laboratory experiments have confirmed that fluid flow in a porous media produces electromagnetic fluctuations (Ishido and Mizutani, 1981). And, anomalies have been detected very clearly at sites around geothermal zones in association with crustal activity. Therefore, it is highly probable that anomalies are generated by water flow changes in the earthquake process and in volcanic occurrences. However, there have been no reports of a high-frequency confined pressure change being detected using a pressure gauge or water level meter. The water vapor temperature at Hodaka did not show any significant fluctuation at the outset of the pipe. It could be understood that the fractured sealing zone (Fenoglio *et al.*, 1995) is generally not hydro-dynamically connected to the sensor, but is only connected electromagnetically, resulting in a unique response to the special electric sensors used in ULEM. The electric signals can be detected at a remote place of several kilometers from the source compared to other physical quantities. In the future, we will have the means to obtain direct supporting evidence of ground water movement.

We attributed the generation mechanism of electric field anomalies to electric-kinetic effects, based on the order estimation of candidates for the cause of self-potential anomalies. The typical signals can be reasonably explained by the confined pressure change of the adoptable properties. However, the MHD mechanism cannot be completely discarded. We may have to investigate geothermal circulation changes in association with magma movement. We limit our discussion here on the mechanisms of generation primarily to demonstrate that the anomalies are physical possibilities under attainable conditions.

We assumed that a confined pressure change is induced by a mechanical rupture of the sealing compartments. However, the disjointed occurrence of earthquakes and electric field anomalies suggests that a pressure change can be induced by a different process. We are reminded of another type of pressure change: vapor collapse in the two-phase flow of water circulation (Ishido and Pritchett, 1999) generating positive polorality. A similar pressure change is assumed around the thermal region of Yellowstone, where the pressure gradient is greater than 147% of the hydrostatic (White *et al.*, 1975) and adiabatic boiling at about 190 m (Fournier, 1969). A temporal pressure change of several mega-pascals could be assumed under these conditions. This will be treated in more detail in the future.

We believe that sufficient documentation for the evaluation of electric field anomalies as precursors of earthquakes has been presented in this article to demonstrate that an electric field anomaly is a true precursor. The phenomena have many useful properties that can be utilized in forecasting earthquakes and volcanic eruptions using ULEM.

Conclusion

An analysis of electromagnetic field variation data obtained by means of an ultra long vertical electric potential measurement (ULEM) around the times of seismic swarms occurrences in central Japan during a period that began in 1989 yielded the following results. :

(1) The electric field anomaly correlates well with seismic swarms as well as volcanic eruptions around the site.

(2) The electric anomaly is caused by electric-kinetic effects induced by variations in the confined water circulation regime.

(3) The selectivity of the signal detection can be attributed to the heterogeneous hydrodymanic and electromagnetic connectivity between the source generation zone and the site.

(4) Pore water pressure changes in the ground water circulation causing earthquakes can be measured using electromagnetic sensors deep underground.

(5) A ULEM especially using well related with underground fluid is the most effective means to detect precursors for use in forecasting earthquakes and volcanic eruptions.

Acknowledgments

We would like to express our thanks to the many people, institutes, and organizations that contributed to this research, especially to Prof. Yukio Hagiwara, Dr. Shigetsugu Uyehara, Dr. Tsuneo Katayama, and Dr. Shigeru Yamane for their encouragement. We thank Prof. Hiroshi Ishii of the Earthquake Research Institue, Prof. Naoyuki Fujii of Nagoya University, Dr. Ryuji Ikeda, Dr. Motoo Ukawa, and Mr. Eiji Yamamoto for their support in our observations. We also thank NEC Corporation ; Nippon Steel Welding Products & Engineering Co., Ltd. ; Tecs. Inc. ; Sankousha Corporation ; Franklin Japan Co., Ltd. ; Izu-Oshima Onsen Hotel ; Teikoku Oil Co., Ltd. ; Nakazato Village of Gifu Prefecture ; Kofu City ; and Shizuoka Prefecture for their helps. Ms. Yamauchi Yumiko contributed in the preparation of the report. We thank Prof. Toshiyasu Nagao and an anonymous referee for reviews and valuable comments.

Reference

Bernard, P., 1992, Plausibility of long distance electrotelluric precursors to earthquakes, *J. Geophys. Res.* **97**, 17531-17546.

Bernard, P. and J.L. Le Mouel, 1996, ed. Lighthill, On electrotelluric signals, a Critical Review of Van earthquake Prediction from Seismic Electrical Signals, World Scientific, 118-129.

Brace, W.F. 1980, Permeability of crystalline and argillaceous rocks, *Int. J. Rock. Mech.* **17**, 876-893.

Byerlee, J., 1993, Model for episodic flow of high pressure water in fault zone before earthquakes, *Geology* **21**, 303-306.

Dobrovolsky, I.P., N.I. Gershenzon and M.B. Gokhberg, 1989, Theory of electrokinetic effects occurring at the final stage in the preparation of a tectonic earthquake, *Phys. Earth Planet. Inter.* **57**, 144-156.

Fenoglio, M.A., M.J.S. Johnston and J.D. Byerlee, 1995, Magnetic and electric fields associated with changes in high pore pressure in fault zones Application to the Loma Prieta ULF emissions, *J. Geophys. Res.* **100**, 12951-12958.

Fitterman, D.V., 1978, Electrokinetic and magnetic anomalies associated with dilatant regions in a layered Earth, *J. Geophys. Res.* **83**, 5923-5928.

Founier, R.O., 1969, Old Faithful : A physical model, *Science* **163**, 304-305.

Fraser-Smith, C.C., C.A. Beernarde, C.P.R. McGill, C.M.E. Ladd, C.R.A. Heeliwell, O. Cand and D.G. Villard, Jr. 1990, Low-frequency magnetic field measurements near the epicenter of the Ms 7.1 Loma Prieta earthquake, *Geophys. Res. Lett.* **17**, 1465-1468.

Fujinawa, Y. 1991, A method for estimating earthquake occurrence probability using first -and multiple- order Markov chain models, *National Hazards* **4**, 7-22.

Fujinawa, Y. and K. Takahashi, 1990, Emission of electromagnetic radiation preceding the Ito seismic swarm of 1989, *Nature* **347**, 376-378.

Fujinawa, Y. and K. Takahashi, 1996, in A Critical Review of VAN (ed. Lighthill, J.) 314-323 (World Scientific, 1996).

Fujinawa, Y. and K. Takahashi, 1998, Electromagnetic radiations associated with major earthquakes, *Phys. Earth Planetary Inter.* **105**, 249-259.

Fujinawa, Y., K. Takahashi and T. Kumagai, 1992, A study of anomalous underground electric field variations associated with a volcanic eruption, *Geophys. Res. Lett.* **19**, 9-12.

Fujinawa, Y., K. Takahashi, T. Matsumoto and N. Kawakami, 1997, Experiments to locate sources of earthquake-related VLF electromagnetic signals, Proc. Japan Acad., 1997, 33-38.

Fujinawa, Y., S. Shimada, S. Ohmi, S. Sekiguchi, T. Eguchi and Y. Okada, 1991, Fixed-Point GPS Observation of Crustal Movement Associated with the 1989 Seismic Swarm and Submarine Volcanic Activities off Ito, Central Japan. *J. Phys. Earth* **39**, 141-153.

Fujinawa, Y. N. Kawakami, J. Inoue, T.H. Asch, S. Takasugi and Y. Honkura, 1999, 2-D georesistivity structure in the central part of the northeastern Japan arc" *Earth Planets and Space,* **51**, 1035-1046.

Fujinawa, Y., K. Takahashi, T. Matsumoto, H. Iitaka, S. Yamane, T. Nakayama, T. Sawada and H. Sakai, 2000, Electromagnetic Field Anomaly Associated with the 1998 Seismic Swarm in Central Japan, *Physics and Chemistry of the Earth*, 25, 247-253.

Fujinawa, Y., T. Matsumoto, K. Takahashi, S. Yamane, H. Iitaka and Y. Enomoto, 2001 a, Spatio-Temporal Relationship between Anomalous ELF/VLF Band Signals and Earthquakes, *Report of National Research Institute for Earth Science and Disaster Prevention,* **61**, 55-81.

Fujinawa, Y., T. Matsumoto, M. Ukawa, H.Iitaka, K. Takahashi, H. Nakano, T. Doi, T. Saito, N. Kasai and S. Sato, 2001 b, Earlier detection of the magma movements by measuring transient streaming potential, Proc. Conduotivity Anomaly Research 18-27.

Fujinawa, Y., T. Matsumoto and K. Takahashi, 2002, Modeling confined pressure changes inducing anomalous electromagnetic fields related with earthquakes, *J. of Applied Geophysics* (to be printed).

Geller, R.J., 1996, ed-1 Debate on evaluation of the VAN Method. Geophys. Res. Lett. 23, 1291-1452.

Gokhberg, M.B., I.L. Gufelf, V.F. Marenko, A.A. Rozhnoy, E. A. Ponomarey and V.S. Yampolsky, 1987, Investigation of disturbances of natural and artificial electromagnetic fields by a source of seismic origin, *Izv. Acad. Sci. USSR, Phys. Solid Earth* U.S.A. **2**, 17-24.

Hayakawa, M. and Y. Fujinawa, 1994, Electromagnetic phenomena related to earth quake prediction, Terra Scientific Pub.

Hickman, S., R. Sibson and R. Bruhn, 1995, Intoduction to special section : Mechanical involvement of fluids in faulting, *J. of Geophys. Res.* **100**, 12831-12840.

Honkura, Y., 1998, On detecting fluid movement in the crust from electromagnetic field variations. *Gekkan Chikyu,* Sup. **20**, 223-225 (in Japanese).

Ingebritsen, S.E. and W., Sanford, 1998, Groundwater in Geologic Processes, *Cambridge Univ. Press.* pp. 341.

Ishido, T. and J.W. Pritchett, 1999, Numerical Simulation of electrotelluric potentials associated with subsurface florid flow, *Geophys. Res. Lett.* **104**, 15247-15259.

Ishido, T. and H. Mizutani, 1981, Experimental and theoretical basis of electrokinetic phenomena in rock-water systems and its applications to geophysics, *J. Geophys. Res.* **86**, 1763-1775.

Lighthill, J., 1996, A Critical Review of Van World Scientific Pub. Co. Ltd.

Majaeva, O., Y. Fujinawa and M.E. Zhitomirsky, 1997, Modeling of Non-Stationary Electrokinetic Effect in a Conductive Crust. *J. Geomag. Geoelectr.* **49**, 1317-1326.

Matsumoto, T., Y. Fujinawa and K. Takahashi, 1996, ULF-bands electric field changes related to seismic swarms. *J. Atmospher. Electri.* **16**, 175-191.

Matsumura, S., Y. Okada, M. Imoto, S. Shimada, S. Hori, T. Ohkubo, M. Ohtake and K. Hamada, 1988, The Functions and Constitutions of the Analyzing System for Precursors of Earthquakes (APE), *The Report of the National Research Center for Disaster Prevention,* **41**, 35-44.

Mizutani, H., T., Ishido, T. Yokokura and S. Ohnishi, 1976, Electrokinetic phenomena associated with earthquakes, *Geophys. Res. Lett.* **3**, 365-368.

Murakami, H., 1989, Geomagnetic Fields Produced by Electrokinetic Sources. *J. Geomag. Geoelectri.* **41**, 221-247.

Nakayama, T., T. Sawada, K. Takahashi and Y. Fujinawa, 1997, Electric field increase preceding the vapor eruption of 1996 at the foot of mount Yakedake. Proc. Conductivity Anomaly Research, 195-201.

Nagao, T., Y. Orihara, T. Yamaguchi, I. Takahashi, K. Hattori, Y. Noda, K. Sayanagi and S. Ueda, 2000, Co-seismic geelectric potentail changes observed in Japan, *Geophys. Res. Lettt.* **27**, 1535.

Nourbehecht, B., 1963, Irreversible thermodynamic effects in inhomogeneous media and their applications in certain geoelectric problems, Mass. Inst. of Technol., Cambridge, Mass.

Overbeek, J.T., 1953, Thermodynamics of electrokinetic phenomena. *J. Colloid Sci.* **8**, 420.

Park, S.K., M.J.S., Johnston, T.R., Madden, F.D. Morgan and F. Morrison, 1993, Electromagnetic precursors to earthquake in the ULF band A review of observations and mechanisms, *Rev. Geophys.* **31**, 117-132.

Parrot, M., J. Achache, J.J. Berthelier, E. Blanc, A. Deschamps, F. Lefeuvre, M. Menvielle, J.L. Plantet, P. Tarits and J.P. Villain, 1993, High-frequency seismoelectromagnetic effects, *Phys. Earth Planet. Inter.* **77**, 65-83.

Poppov, L.N., Y.K., Krakovetzkiy, M.B. Gokhberg and V.A. Pilipenko, 1989, Terrogenic effects in the ionosphere a review, *Phys. Earth Planet. Inter.* **57**, 115-128.

Raiche, A.P., 1974, An integral equation approach to three-dimensional modelling, *Geophys. J.R. astr. Soc.* **36**, 363-376.

Rakityansky, I.I., 1982, Geoelectromagnetic Investigatin of the Earth's Crust and Mantle Springer-Verlag, Berlin.

Rikitake, T., 1976, Earthquake Prediction, Elsevier, New York, 357 pp.

Scholz, C.H., 1990, The mechanics of earthquakes and faulting, Cambridge University Press, 276 pp.

Surkov, V.V., S. Uyeda, T. Nagao and M. Hayakawa, 2001, Fractal roperties of seismoelectric phenomena., *J. Geodinamics,* (in press).

Takahashi, H. and K. Takahashi, 1989, Tomography of seismo-radio wave source regions for predicting imminent earthquakes, *Phys. Earth and Planetary Inter.* **51**, 40-44.

Takahashi, H., Y. Fujinawa, T. Matsumoto, T. Nakayama, T. Sawada, H. Sakai and H. Iitaka, 2000, Underground electric field observation at Hodaka Station 1993-1999, *Report of National Research Institute for Earth Science and Disaster Prevention* **204**, 1-224.

Utsu, T., 1983, Probabilities associated wit earthquake prediction and their relationships, *Earthquake Prediction Res.* **2**, 105-114.

Varotsos, P. and M. Lazaridou, 1991, Latest aspects on earthquake prediction in Greece based on seismicelectric signals, *Tectonophysics* **188**, 321-347.

Varotsos, P., M. Lazaridou, K. Eftaxias, G. Antonopoulos, J. Makris, J. Kopanas, 1996, in A critical review of VAN ed. Lighthill, J. 29-76 World Science Publishing Co., Ltd., Singapore.

Wakita, H., Y. Sano and M. Mizoue, 1987, High 3He emanation and seismic swarms observed in a nonvolcanic, forearc region, *J. Geophys. Res.* **92**, 12539-12546.

Weidelt, P., 1975, Electromagnetic induction in three-dimensional structures, *J. Geophys.* **41**, 85-109.

White, D.E., R.O. Fournier, L.J.P. Muffler and A.H. Truesdell, 1975, Physical results of research drilling in thermal areas of Yellowstone National Park, Wyoming. *U.S. Geological Survey Profesional Paper* **892**.

Wyss, M., 1991, Evaluation of Proposed Earthquake Precursors, AGU, Washington, D. C. pp 94.

Wyss, M. and D.C. Booth, 1997, The Iaspei procedure for the evaluation of earthquake precursors, *Geophys. J. Internat.* **131**, 423-424.

Yoshida, S., M. Uyeshima and M. Nakatani, 1997, Electric potential changes associated with slip failure of granite : Preseismic and coseismic signals, *J. Geophys. Res.* **103**, 14883-14897.

Yoshida, S., O.C. Clint and P.R. Sammonds, 1998, Electric potential changes prior to shear fracture in dry and saturated rocks, *Geophys. Res. Lett.* **25**, 1577-1580.

Zlotnicki, J. and J.L. Le Mouel, 1990, Possible electrokinetic origin of large magnetic variations at La Fournaise Volcano, *Nature* **343**, 633-636.

Zhao, D. and H. Negishi, 1998, 1995 Kobe earthquake : Seismic image of the source zone and its implications for the rupture nucleation, *Journal of Geophysical Research* **103**, B5, 9967-9986.

(Received July 13, 2001)
(Accepted October 18, 2001)